

Ship Hull Plating Weld Misalignment Effects when Subjected to Tension

by

M. Cameron Weaver

B. S. Mechanical Engineering  
California Polytechnic State University San Luis Obispo, 1986

Submitted to the Department of Ocean Engineering and  
the Department of Mechanical Engineering  
in partial fulfillment of the requirements for the degree of

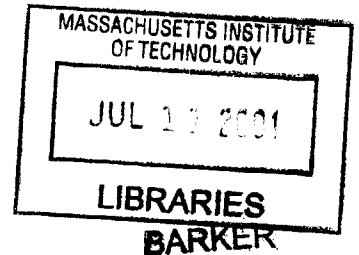
Master of Science in Naval Architecture/Marine Engineering

And

Master of Science in Mechanical Engineering


At the

MASSACHUSETTS INSTITUTE OF TECHNOLOGY  
June 2001




© 2001 Massachusetts Institute of Technology  
All rights reserved

Signature of Author.....

  
Department of Ocean Engineering and  
The Department of Mechanical Engineering  
11 May 2001


Certified by.....

  
Tomasz Wierzbicki  
Professor of Applied Mechanics  
Thesis Supervisor

Certified by.....

  
Frank A. McClintock  
Professor of Mechanical Engineering  
Thesis Reader

Accepted by.....

  
Professor Ain A. Sonin  
Chairperson, Department Committee on Graduate Students  
Department of Mechanical Engineering

Accepted by.....

  
Professor Henrik Schmidt  
Professor of Ocean Engineering  
Chairperson, Department Committee on Graduate Students

# Ship Hull Plating Weld Misalignment Effects when Subjected to Tension

by

M. Cameron Weaver

Submitted to the department of Ocean Engineering and  
the Department of Mechanical Engineering  
on 11 May 2001, in partial fulfillment of the  
requirements for the degree of  
Master of Science of Naval Architecture and Marine Engineering  
and  
Master of Science in Mechanical Engineering

## Abstract

Precision fabrication of ships is advancing. Welding is ubiquitous in ship construction and military standards have specified tolerances for joining plates in naval combatants. Precision manufacturing will allow the production of ships with smaller hull plate misalignments. A benefit from this could be improved ship survivability when subjected to underwater explosions. Slip Line Fracture Mechanics interacting with Finite Element Analysis (FEA) gives insight into the deformation, necking and fracture mechanisms of typical over-matched welds. The weld rotates with local necking until the plates are aligned and then shears off.

FEA showed the importance of deformed geometry in promoting final fracture by slip from the toe of the weld in non-hardening material. Graphical results indicate that for a non-hardening material with an offset of 15% of the plate thickness, which is within current military standards, weld rotation of 4-6° and local plate thinning of 4-5% in the region next to the weld can be expected. A test specimen showed a 4° weld rotation but did not provide the plane-strain condition and failed by necking away from the weld. A re-design is suggested.

Thesis Supervisor: Tomaz Wierzbicki  
Title: Professor of Applied Mechanics

Thesis reader: Frank A. McClintock  
Title: Professor of Mechanical Engineering

## Table of Contents

<b>Abstract.....</b>	<b>2</b>
<b>List of Figures.....</b>	<b>4</b>
<b>List of Tables .....</b>	<b>4</b>
<b>Chapter 1 Introduction.....</b>	<b>5</b>
1.1 Need .....	5
1.2 Prior Work .....	7
<b>Chapter 2 Slip Line Analysis .....</b>	<b>9</b>
2.1 Statement of Problem.....	9
<b>Chapter 3 Slip Line Field Theory.....</b>	<b>11</b>
3.1 Assumptions.....	11
<b>Chapter 4 Graphical Integration.....</b>	<b>20</b>
4.1 Application of slip line field theory .....	20
<b>Chapter 5 Finite elements .....</b>	<b>27</b>
5.1 Finite Element Approach .....	27
<b>Chapter 6 Experiments.....</b>	<b>32</b>
6.1 Specimen design .....	32
6.2 Testing procedure and apparatus .....	34
<b>Chapter 7 Analysis of test data .....</b>	<b>37</b>
7.1 Results.....	37
7.2 Conclusions.....	41
7.3 Recommendations for Further Study .....	41
<b>Bibliography .....</b>	<b>43</b>
<b>Appendix A Specimen calculations .....</b>	<b>44</b>
<b>Appendix B Flat plate specimen test data.....</b>	<b>45</b>
<b>Appendix C Offset specimen test data .....</b>	<b>50</b>

## List of Figures

Figure 1. Transom module construction [1].	5
Figure 2. Finished horizontal welded joints [1].	6
Figure 3. Plate offset.	6
Figure 4. Geometry of a welded joint (weldment).	10
Figure 5. EH-36 weld hardness profile [9].	10
Figure 6. Stress-strain curves of an actual vs. rigid-perfectly plastic material.	12
Figure 7. Element orientation on free surface.	13
Figure 8. Free-body diagram of weldment. (Cross-sectional view)	16
Figure 9. Neutral axis position as a function of plate offset.	17
Figure 10. Displacements along $\alpha$ and $\beta$ -lines.	17
Figure 11. Initial weldment geometry (dimensions in cm).	21
Figure 12. Rigid body rotation mechanics.	22
Figure 13. Sequence for 1 degree clockwise weld rotation.	23
Figure 14. Weldment rotation to remove offset.	24
Figure 15. Weldment rotation to equilibrium.	24
Figure 16. Top surface strain increments per degree of clockwise weld rotation.	26
Figure 17. ABAQUS <sup>®</sup> mesh of offset plates [13].	29
Figure 18. ABAQUS <sup>®</sup> displacement to onset of plasticity [13].	30
Figure 19. ABAQUS <sup>®</sup> showing slip line fields and shear bands [13].	31
Figure 20. 16.7% offset test specimen drawing (dimensions in inches).	33
Figure 21. Cross-section of offset specimen showing the line of action.	33
Figure 22. Test set-up of flat plate specimen. (Only one extensometer shown).	35
Figure 23. 16.7% offset test specimen set-up.	36
Figure 24. Stress-strain curve for the flat plate "dog-bone" specimen.	38
Figure 25. Stress-strain curve for specimen with 16.7% offset.	39
Figure 26. 16.7% offset specimen rotation.	40

## List of Tables

Table 1. Allowable butt weld offsets [7].	8
Table 2. Calculated strains as a fraction of plate thickness per degree of clockwise rotation of rigid weld.	25
Table 3. Summary of observed properties of EH-36 specimens.	38
Table 4. Comparison of test results to slip line field theory predictions.	40

## Chapter 1 Introduction

### 1.1 Need

The Office of Naval Research (ONR) has a keen interest in the possible applications of precision manufacturing of ship hull structures. The United States Navy is exploring the use of precision manufacturing for future shipbuilding. This research addresses the possible benefits of precision welding with reduced misalignments when ship hull plates are subjected to an underwater explosion (UNDEX). Misalignment could either be angular or plate offset. Offset of the plates will be the kind studied in this paper.

Offsets in welds can easily arise in welding sections with beams of 10 m and 10 mm hull plating (see Figure 1). Figure 2 shows the visible welded joints of a finished combatant.

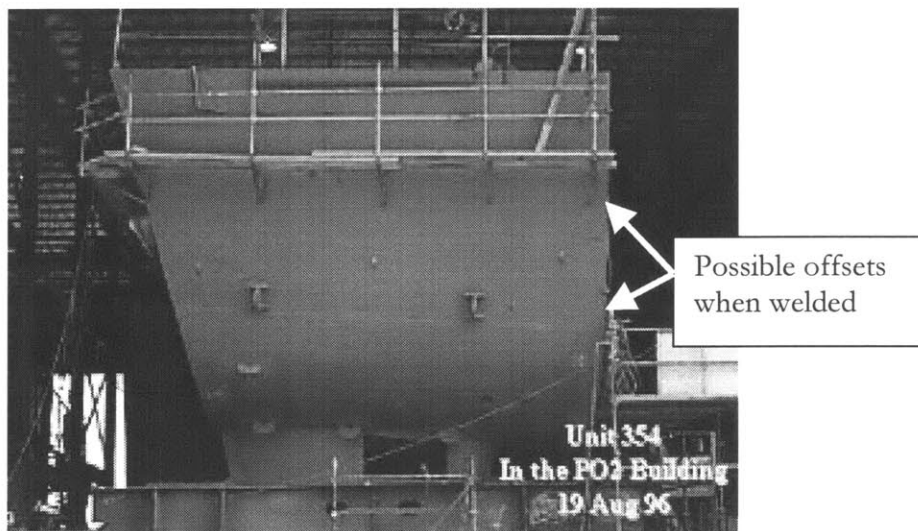


Figure 1. Transom module construction [1].

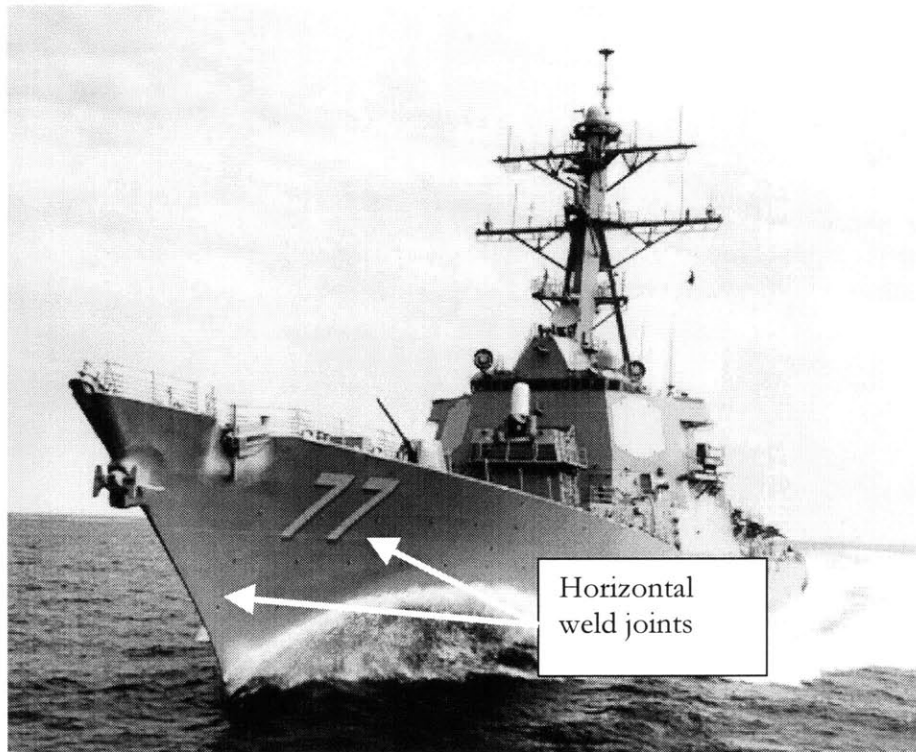


Figure 2. Finished horizontal welded joints [1].

Figure 3 shows the geometry of ship hull plating with an offset for a typical welded joint of the kind that will be explored in this research.

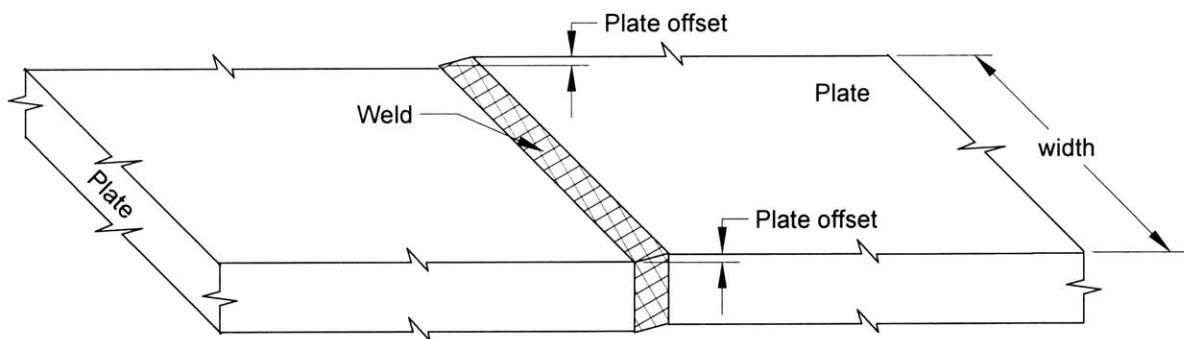


Figure 3. Plate offset.

## 1.2 Prior Work

Extensive research has addressed the strength of weldments in ship hull plating, but none were found on the effect on the offset on the tensile behavior. For example Ship Structural Committee Report, SSC-4, by Snelling (1946) [2], addressed the effects on welded plates when subjected to explosions; however, the specific problem of plate misalignment was not characterized or explored. As reference for future research into this effect of UNDEX, Ship Structural Committee Report, SSC-6, Davis (1948) [3], et al., investigated the fracture of welded flat plates by subjecting them to a bend test simulating explosions. Ship Structural Committee Report, SSC-335, by Dexter (1986) [4], et al., had good hardness profiles from underwater welding. This result was compared with data obtained from welding EH-36 in air. Nguyen (1998) [5], et al., studied the effect of weld geometry and fatigue characteristics due to the welds. Plate angular misalignment and offset affects under compression were studied by Cui (1999) [6], et al.. In conclusion, the plethora of papers published about welded plates has failed to quantify the effect of plate misalignment when the plate is subjected to tension

The perfect alignment of plating on such a large scale as a ship's hull is difficult. Military standards concerning plate offset have been developed. Table 1 shows the accepted tolerances for butt welds.

Table 1. Allowable butt weld offsets [7].

Plate Thickness (in)	Allowable Offset (in)	Allowable Offset %
Less than 3/8	1/16	≥16.67 %
3/8 to 3/4	1/8	16.67 – 25 %
over 3/4 to 1-1/2	3/16	12.5 – 25 %
over 1-1/2	1/4	≤16.67 %

Typical ship building practices produce no more than 1/16 of an inch offset regardless of the thickness of the plate welded [8]. However, localized offsets can be at the maximum allowed in Table 1. An offset of 15% of the plate thickness was used throughout this paper as a reasonable compromise.



## Chapter 2 Slip Line Analysis

### 2.1 Statement of Problem

To reduce cost of the new class of Amphibious Assault ship (LPD-17), the U. S. Navy has opted to use commercial grade steel, a “mild” steel, EH-36. The characteristics of EH-36 steel have been studied extensively. For strength in welded joints, the hardness of a weld is greater than the base metal (over-matching). The volume between the weld and the base metal is called the heat-affected zone (HAZ) as shown in Figure 4, where  $h$  is the plate thickness and  $m$  is the fraction of the plate thickness corresponding to the offset. Being next to the base metal it is cooled rapidly and is harder (see Figure 5).

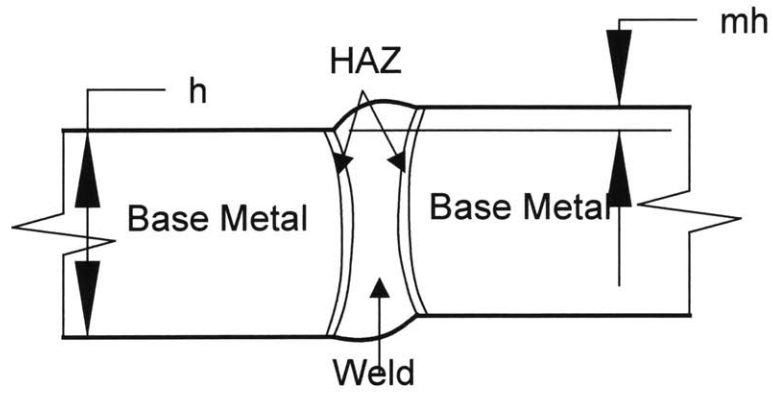


Figure 4. Geometry of a welded joint (weldment).

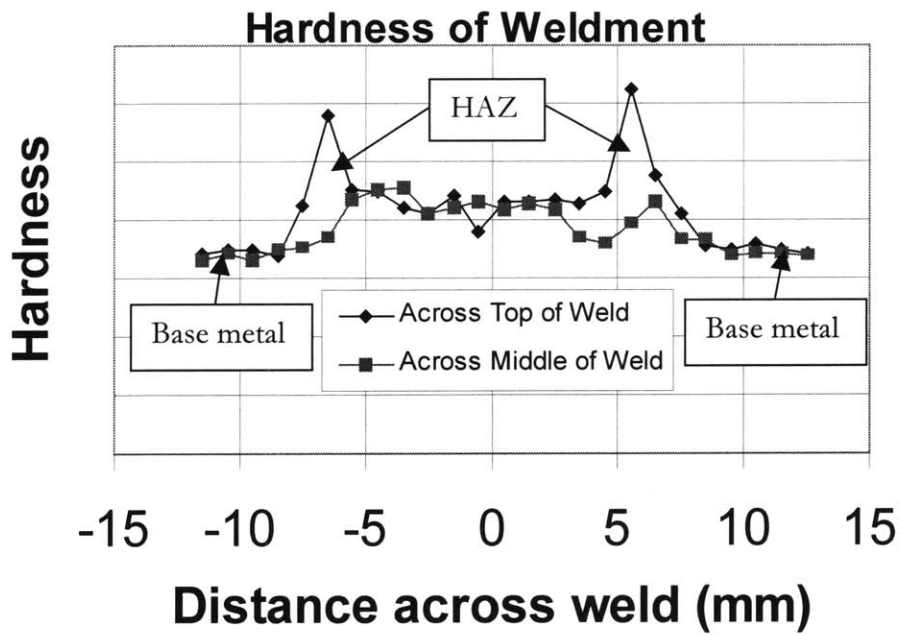


Figure 5. EH-36 weld hardness profile [9].

## **Chapter 3 Slip Line Field Theory**

### **3.1 Assumptions**

The loading of the ship plating when subjected to an UNDEX is a dynamic event. However, for local analysis, quasi-static equilibrium conditions will be assumed. This is justified by the nature of the critical damage caused by an UNDEX, extending over many plate thicknesses, perhaps up to a few frame spacings. The time for such damage to develop is large compared to that for spall fracture or shearing at supports. This time is sufficient for the stress wave to travel through the plate thickness many times, establishing local quasi-static equilibrium.

A rigid-perfectly plastic material will be assumed (see Figure 6) during the application of slip line field theory. This is considered accurate because elastic strain at yield for typical structural steel is on the order of 0.2% [10]. Therefore, for the deformation taken well into plasticity, elastic strains can be neglected. The strain before fracture due to an UNDEX are large compared to its elastic strain.

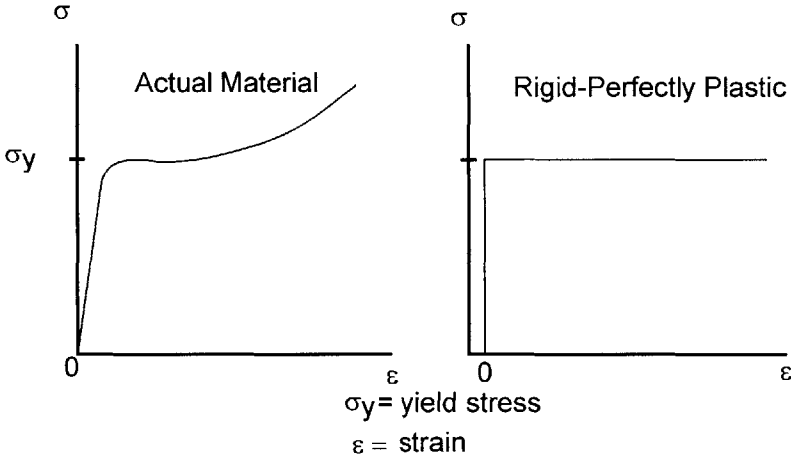


Figure 6. Stress-strain curves of an actual vs. rigid-perfectly plastic material.

Since the normal ship building practice is to have the weld over-matched, it is reasonable to assume the weld and heat-affected zone as being a rigid body. The width of the HAZ is small when compared to the plate thicknesses under consideration [11], so its width will be assumed to be negligible and lumped into the weld. In this rigid-perfectly plastic model, in plasticity, the material is homogenous and stress throughout it is constant and equal to the yield stress,  $\sigma_y$  or  $2k$ . The following summarizes the assumptions to be used:

- a. Plane strain

- b. Non-hardening material
- c. Rigid-perfectly plastic material behavior
- d. Uniform stress under a free surface - as a consequence in a deforming region.

The following treatment is taken from McClintock (2000) [12]. In a region on the top surface, presumably deforming in tension, two elements are drawn adjacent to the top surface at points A and B in Figure 7. There is no traction acting on the free surface. Therefore, the normal stress,  $\sigma_{yy}$ , and the shear stress,  $\sigma_{xy}$ , are zero.

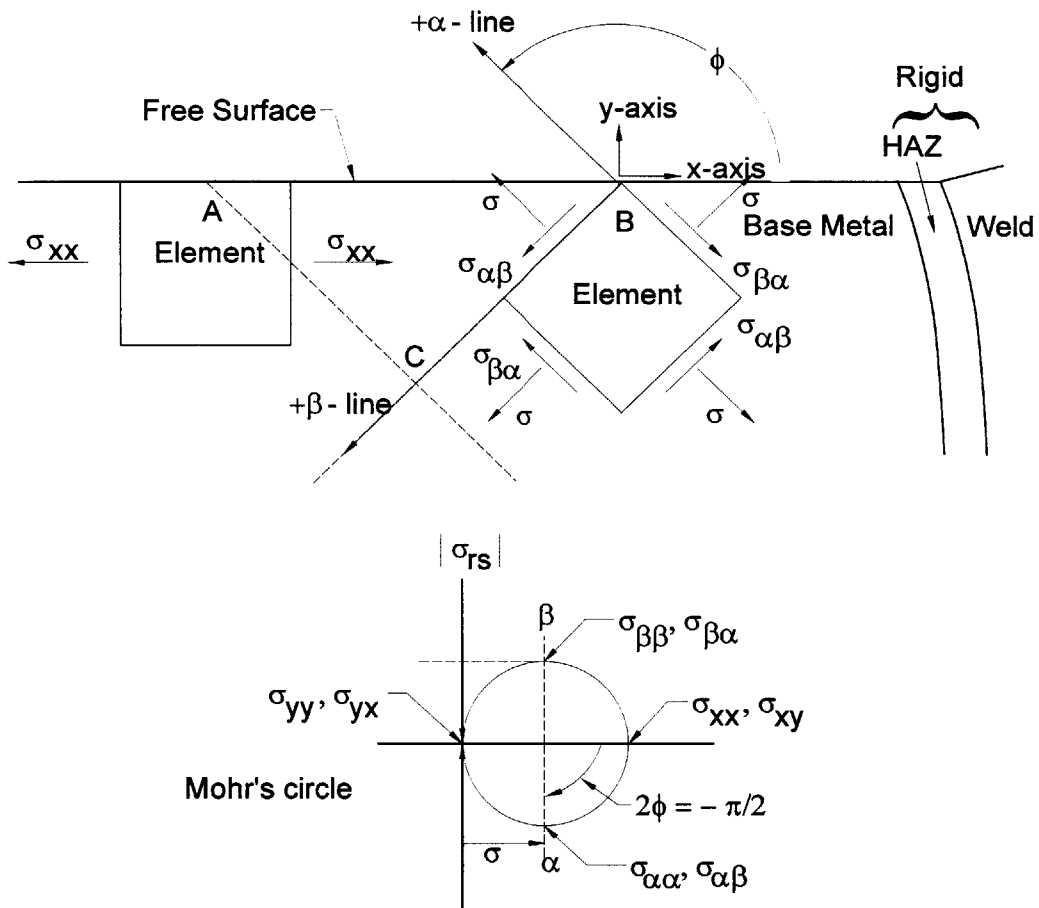


Figure 7. Element orientation on free surface.

In the x-direction stress,  $\sigma_{xx}$ , develops due to a far field tensile force and is given the value of  $2k$ . Mohr's circle is also drawn in Figure 7 using these boundary conditions and reveals a maximum shear stress,  $k$ , at  $\pm 45^\circ$  from the free surface. The radius of Mohr's circle is constant at  $k$  for this plane-strain non-hardening situation.

The orthogonal coordinates, shown in Figure 7, parallel to the planes of maximum shear and are called  $\alpha$ -lines and  $\beta$ -lines. Along these two lines plastic flow, or slip, can take place. They are oriented such that the axis of maximum principle stress is  $45^\circ$  counter-clockwise from the  $\alpha$ -line toward the  $\beta$ -line. This orientation will remain constant at these angles from the free surface throughout this analysis. The angle counter-clockwise from the x-axis to the  $\alpha$  slip line is denoted by  $\phi$ .

The Cartesian components of stress are:

$$\sigma_{xx} = \sigma - k \sin 2\phi \quad (1a)$$

$$\sigma_{yy} = \sigma + k \sin 2\phi \quad (1b)$$

$$\sigma_{xy} = k \cos 2\phi \quad (1c)$$

where  $\sigma_{xx}$  and  $\sigma_{yy}$  are the normal stresses,  $\sigma_{xy}$  is the shear stress,  $\sigma$  is the mean normal stress.

Along the two slip lines, the in-plane partial differential equations of equilibrium become:

$$\text{Along an } \alpha\text{-line, } d\sigma = 2k d\phi \quad \text{and} \quad (2)$$

$$\text{along a } \beta\text{-line, } d\sigma = -2k d\phi. \quad (3)$$

Integrating inward along an  $\alpha$ -line from point A to point C yields,

$$\sigma_C - \sigma_A = 2k(\phi_C - \phi_A). \quad (4)$$

Since the angle,  $\phi$ , at both point A and C is  $45^\circ$  counter-clockwise from the x-axis and constant, the stress at point C,  $\sigma_C$ , is equal to the stress at point A,  $\sigma_A$ . Similarly, integrating inward from point B to point C along a  $\beta$ -line yields,

$$\sigma_C - \sigma_B = -2k(\phi_C - \phi_B). \quad (5)$$

Again,  $\phi$  is constant resulting in the stresses at points B and C,  $\sigma_B$  and  $\sigma_C$  respectively, being equal. When this process is repeated to additional points into the material, the same results are found. It is also discovered that when reaching the bottom free surface the signs of the stresses are reversed. Performing this process starting from the bottom free surface yields the same sign discontinuity when reaching the top surface. It is clear there are two active slip line fields that approach a neutral axis.

Considering the overall equilibrium, applying a displacement,  $u$ , to the plate ends, a far field tensile force,  $P$ , operates through the center of the weld (see Figure 8). Summing the forces in the x-direction and moments about point O, yields Equations (6) and (7) respectively. Assuming the width (recall Figure 3) of the plate to be unity, and setting both of them equal to zero to satisfy equilibrium:

$$\sum F_x = -P + 2k(h - y_{na}) - 2ky_{na} = 0 \quad (6)$$

$$\sum M_o = -P \left( \frac{1}{2} h + y_p - y_{na} \right) + \frac{1}{2} 2ky_{na}^2 + \frac{1}{2} 2k(h - y_{na})^2 = 0 \quad (7)$$

where  $2k$  is the yield stress of the metal,  $h$  is the thickness of the plate,  $y_{na}$  is the position of the neutral axis from the bottom surface, and  $y_p$  is the distance of the offset from the applied tensile force,  $P$ , to the center of the cross-section of the plate.

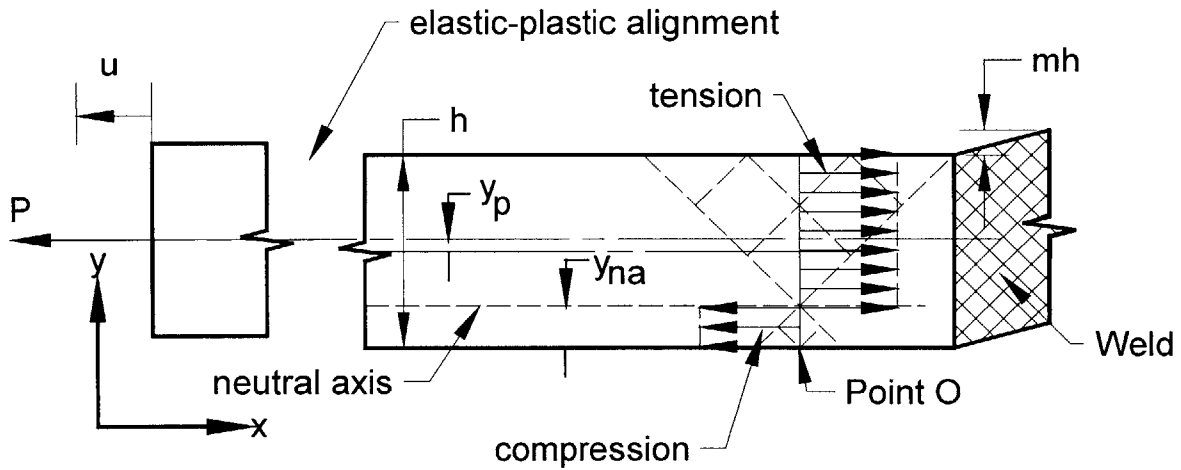


Figure 8. Free-body diagram of weldment. (Cross-sectional view)

Expanding and substituting Equation (6) into Equation (7) yields Equation (8), a solution for the position of the neutral axis as a function of the plate offset,  $m$ . Figure 9 shows the relationship.

$$y_{na} = \frac{1}{2} (h + 4mh - \sqrt{h^2 + 16m^2 h^2}) \quad (8)$$



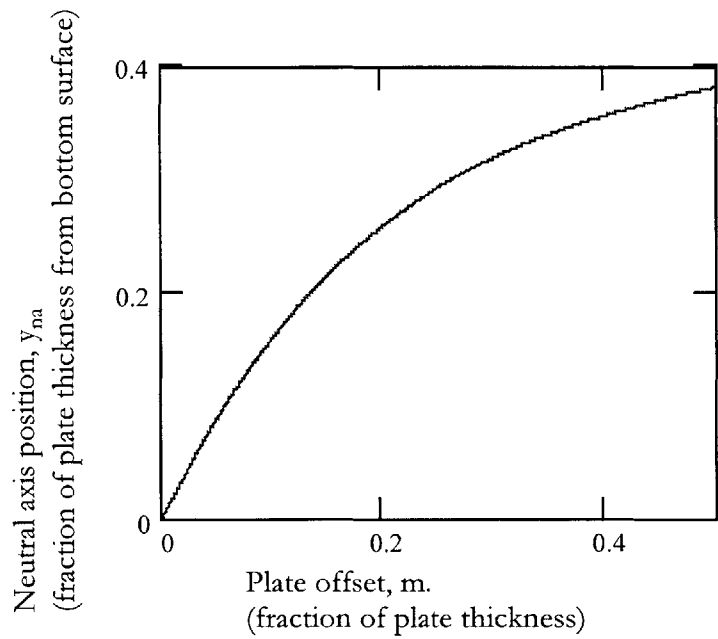


Figure 9. Neutral axis position as a function of plate offset.

The displacement increments, or “velocities” in terms of a fictitious time, are denoted  $u_\alpha$  and  $u_\beta$  along the  $\alpha$ -lines and  $\beta$ -lines respectively and shown in Figure 10.

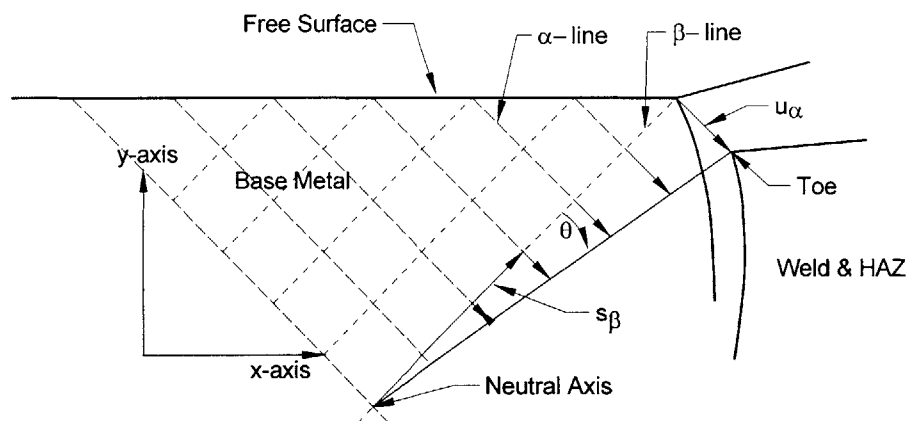


Figure 10. Displacements along  $\alpha$  and  $\beta$ -lines.

The partial differential equations of incompressibility lead to:

Along an  $\alpha$ -line;

$$du_{\alpha} = u_{\beta} d\phi \quad \text{and} \quad (9)$$

along a  $\beta$ -line;

$$du_{\beta} = -u_{\alpha} d\phi. \quad (10)$$

Shear discontinuities are possible across an  $\alpha$ -line (along a  $\beta$ -line) so there is no limit to the change in  $u_{\alpha}$ . Similarly, across a  $\beta$ -line,  $u_{\beta}$  can change discontinuously.

Knowing  $\phi$  is a constant,

$$d\phi = 0. \quad (11)$$

This yields from equation (9),

$$du_{\alpha} = 0. \quad (12)$$

Therefore along an  $\alpha$ -line  $u_{\alpha}$  is a constant and has a solution;

$$u_{\alpha} = s_{\beta} \theta \quad (13)$$

where  $s_{\beta}$  is the distance along a  $\beta$ -line and  $\theta$  is the small, displaced angle of the  $\beta$ -line.

Recalling equation (10), along a  $\beta$ -line:

$$du_{\beta} = -u_{\alpha} d\phi. \quad (10)$$

Applying the boundary condition that the toe of the weld is rigid due to its higher hardness, at the end of the  $\beta$ -line shown in Figure 10, no change in length is allowed so,

$$u_{\beta} = 0. \quad (14)$$

Therefore, there is no displacement,  $u_{\beta}$ , along any  $\beta$ -line. This conclusion will be used during the graphical solution to give insight into the deformation and failure mechanisms of the welded plates in question.

## **Chapter 4 Graphical Integration**

### **4.1 Application of slip line field theory**

DELTA CAD<sup>®</sup> software is employed for improved accuracy to the graphical solution. The line of action of the applied external force  $P$ , imposes a moment that rotates the weld. This removes some of the offset, shifting the neutral axis down, and causing the resulting stress components along the rigid body interface closer to a line of action through the center of the weld. Figure 11 shows the initial geometry of a plate with 15% of the plate thickness offset.

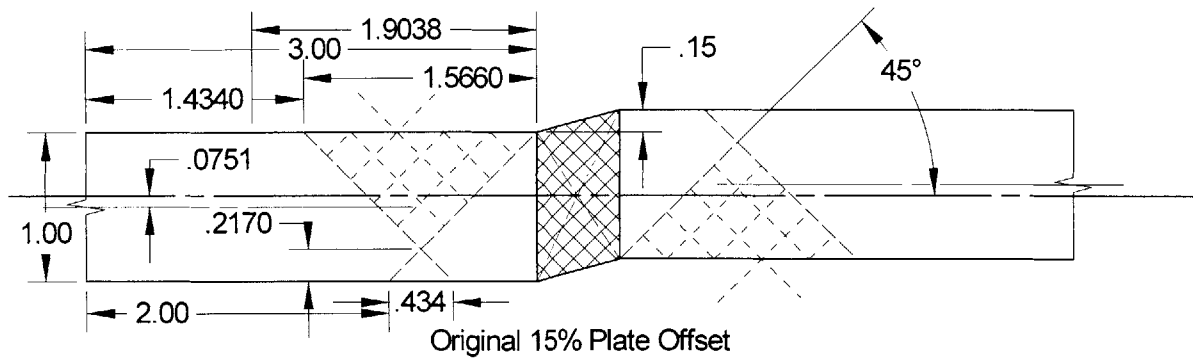


Figure 11. Initial weldment geometry (dimensions in cm).

The crosshatched area is the weld and a region of rigidity. The dashed lines indicate slip line fields ( $\alpha$ -lines and  $\beta$ -lines). Choosing weld rotation as the variable, increments of 1 degree are sequentially mechanically imposed to the weld with the center of the weld fixed. The upper triangle is in tension and slip occurs along the  $\alpha$ -lines only. The lower triangle is in compression and again slip only occurs along the  $\alpha$ -lines. Solving Equations (9) and (10) with the applied boundary conditions yields the quasi-static rigid body shapes as seen in Figure 12. Applying a displacement,  $u$ , to the far field end of the plate, a tensile force develops. This moves rigid body E to the left and upwards with no rotation. A hinge at point F imposes a rotation on rigid body D about its center.

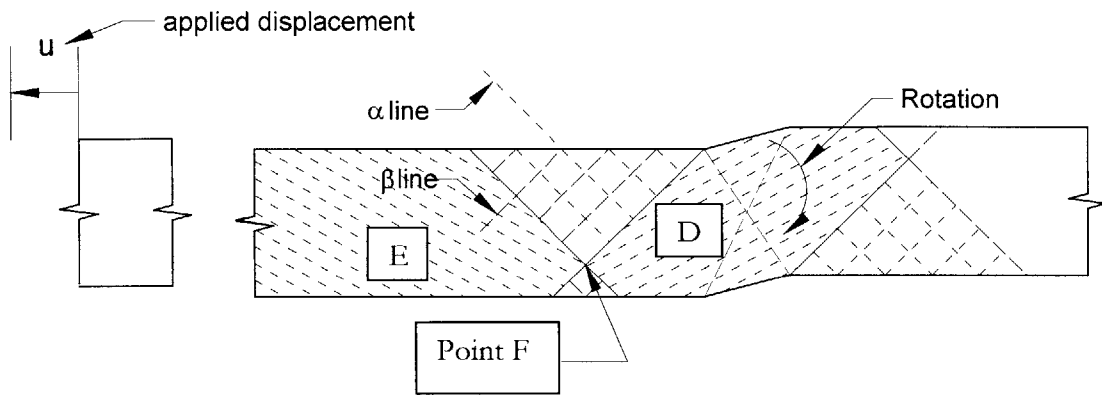


Figure 12. Rigid body rotation mechanics.

The same phenomenon is mirrored and upside down on the other side of the weld. Each incremental rotation causes the offset to become less while the neutral axis moves toward the lower surface. Note: It is recognized that fans of slip line fields will arise as the body deforms. The shape assumed for rigid body D during this analysis is driven by the solution derived in chapter 3. Again, the only rigid region of rigid body D is the weld itself. All other regions of rigid body D are free to deform. This treatment is considered a good upper bound approximation.

Figures 13 shows a representative sequence of events required when the weld is rotated 1 degree clockwise. It is assumed the deforming top and bottom surfaces remain straight. However, since the neutral axis is shifting down, the affected top surface becomes

longer, resulting in a small curved section at the left end of the slip line field shown. This affect is considered small and negligible.

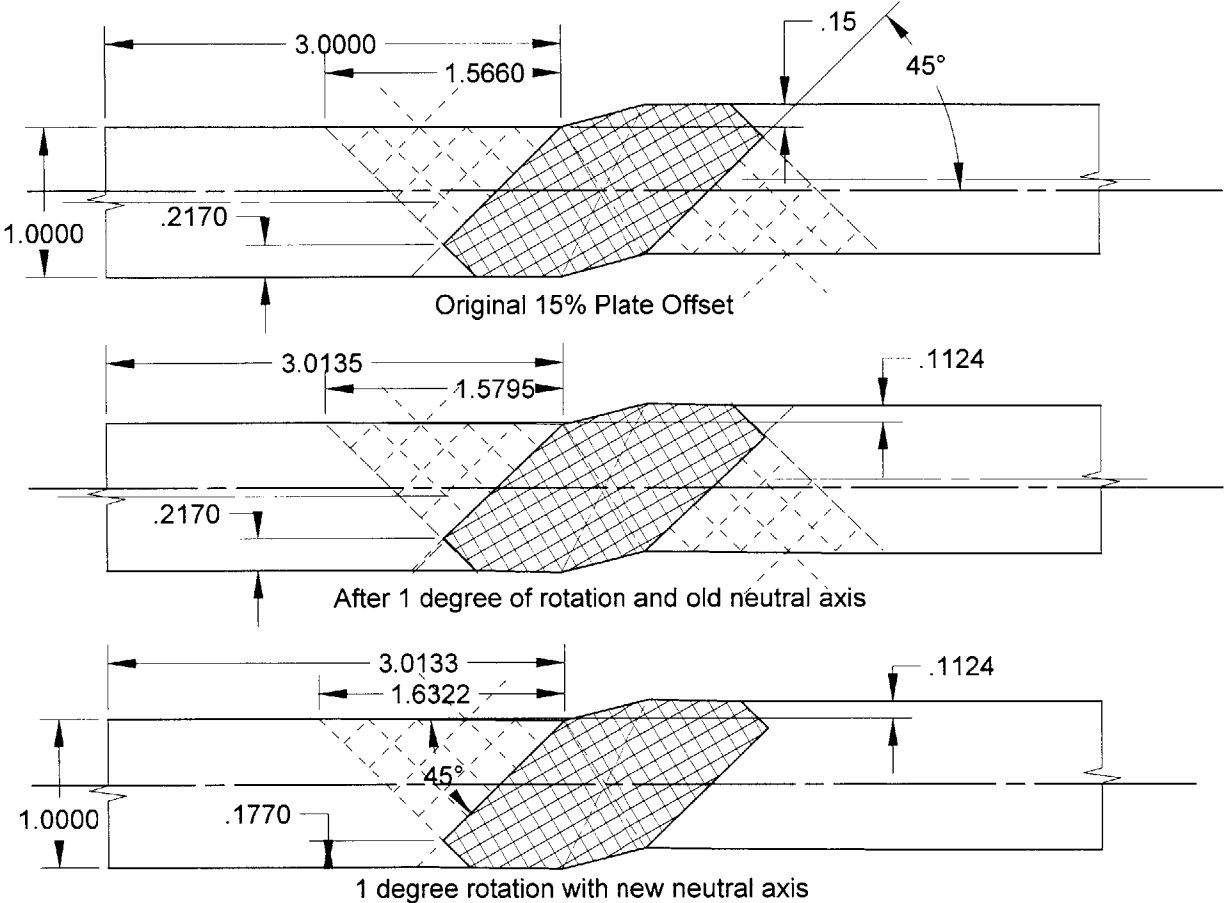


Figure 13. Sequence for 1 degree clockwise weld rotation.

Figure 14 shows the weldment after about 4 degrees of clockwise rotation. The offset is removed.

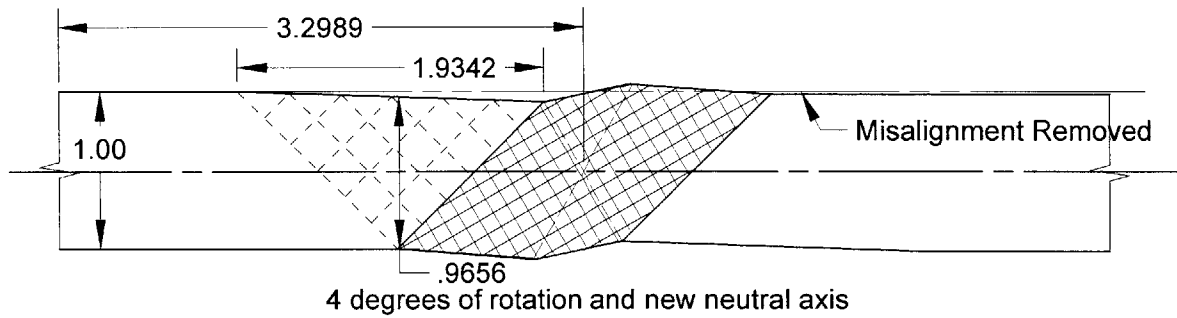


Figure 14. Weldment rotation to remove offset.

It is evident that some thinning occurs in the region next to the weld. However, the resulting stresses acting on the interface between the slip line field and the weld are not yet in equilibrium. The center of the slip line face in the slip field is lower than the center of the weld. Further rotation of the weld is necessary to reach equilibrium as Figure 15 shows.

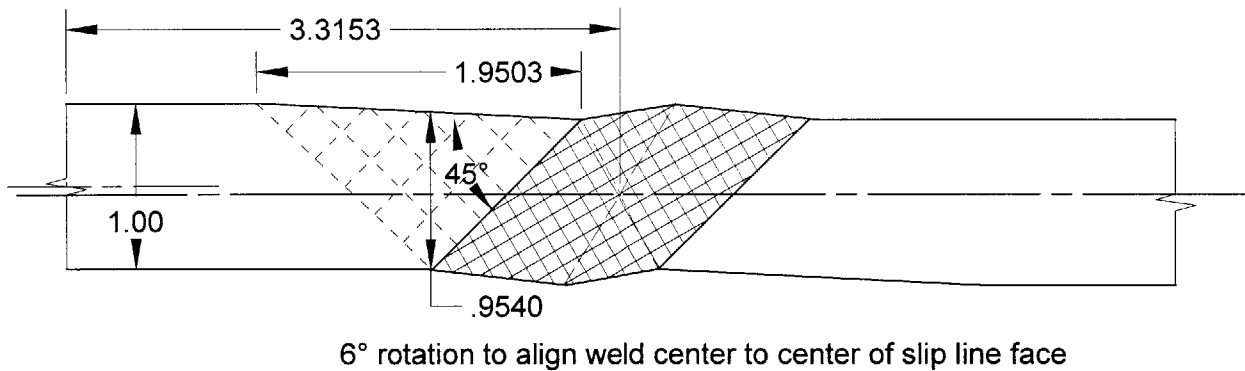


Figure 15. Weldment rotation to equilibrium.

At this angle of weld rotation, about 6 degrees clockwise, the resulting stresses on the interface plane between the slip line plane and rigid body D act through the center of



the weld. The plastic strains observed along the top surface in the x-direction ( $\epsilon_{xx}$ ) are displayed in Table 2 and graphed in Figure 16. A linear trend line was added using the method of least squares to smooth out the results of the graphical approach.

Table 2. Calculated strains as a fraction of plate thickness per degree of clockwise rotation of rigid weld.

Weld Rotation (degrees CW)	Calculated strain (incremental $\epsilon_i$ )
1	0.00683
2	0.00706
3	0.00737
4	0.00778
6	0.00815

This amount of plastic strain is believed to lead to a shear band emanating from the toe of the weld down to the bottom surface at about a 135 degree clockwise angle from the x-axis. Shearing off of this surface cannot happen until the neutral axis vanishes and the entire cross section is experiencing tension promoting this shear band. The addition, summed up by Equation (14), of all the plastic strains observed while applying slip line field theory and rigid body kinematics along the top surface next to the weld is 0.037 or 3.7%.

$$\epsilon = \sum_{i=1}^6 \epsilon_i = 0.037 \tag{14}$$

### Top Surface Strains vs Rotation

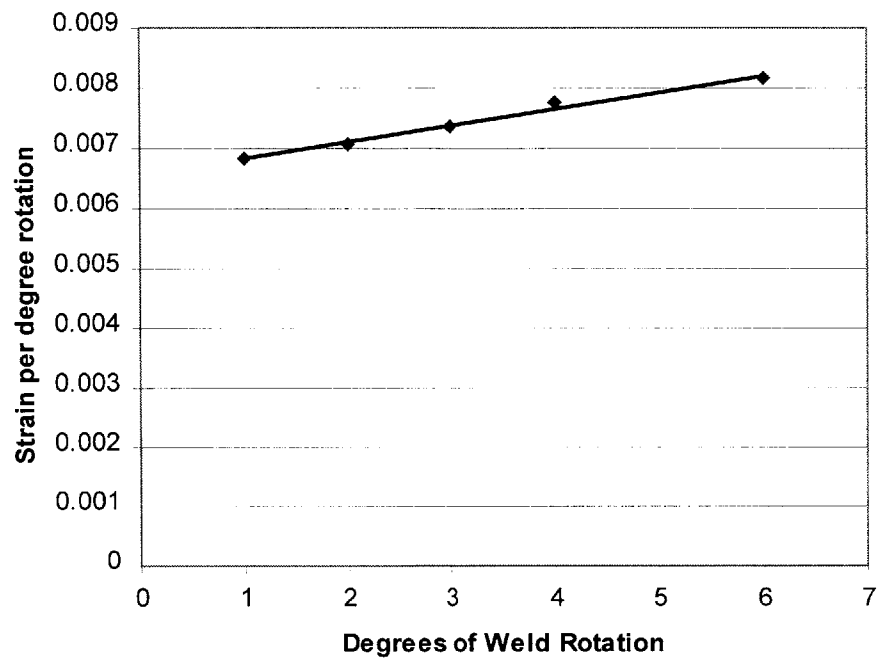


Figure 16. Top surface strain increments per degree of clockwise weld rotation.

## Chapter 5 Finite elements

### 5.1 Finite Element Approach

In addition to the slip line field solution based on a rigid-perfectly plastic model, Teng (2001) [13] conducted finite element analysis. The following properties of the base metal and weld metal were assumed:

Base metal- Modulus of Elasticity,  $E = 200,000$  MPa

Upper Yield Point, UYP = 200 MPa

Poisons ratio,  $\nu = 0.48$

Weld metal- Modulus of Elasticity,  $E = 200,000$  MPa

Upper Yield Point, UYP = 260 MPa

Poisons ratio,  $\nu = 0.48$ .

These values were chosen to mimic a rigid-perfectly plastic, nearly incompressible, model. A displacement was applied at each end of the model while the center of the weld was fixed. Figure 17 shows the mesh selected in the region of the offset. A mesh density of twenty elements through the thickness was used for the weld and adjacent regions. To reduce the CPU time, the mesh density was lowered to ten and then six elements through the thickness at 5 and 10 plate thicknesses away from the center, respectively. This mesh is sufficiently fine enough to capture the expected compression zone near the weld. The output from ABACUS<sup>®</sup>, Figure 18, shows the plastic strain in the x-direction, pe11, resulting from a displacement imposed at the plates free ends corresponding to the strain required to induce plasticity of 0.03 compared to the elastic strain of 0.003. The position of neutral axes are clearly visible. An additional displacement was applied to induce a plastic strain of 0.1. The slip line field is evident as the triangular regions in Figure 19. The entire cross-section is now in tension, forming a shear band from the toe of the weld and extending to the bottom surface at approximately a 135 degree clockwise angle from the positive x-axis.

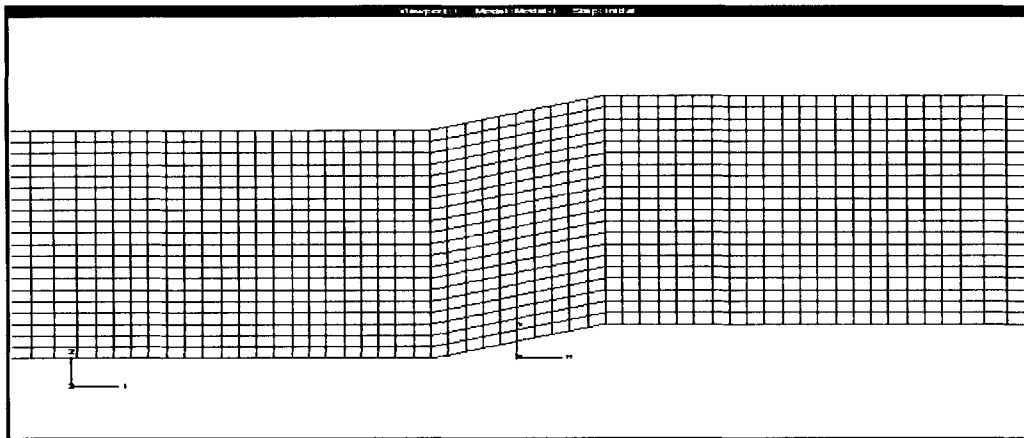


Figure 17. ABAQUS<sup>®</sup> mesh of offset plates [13].

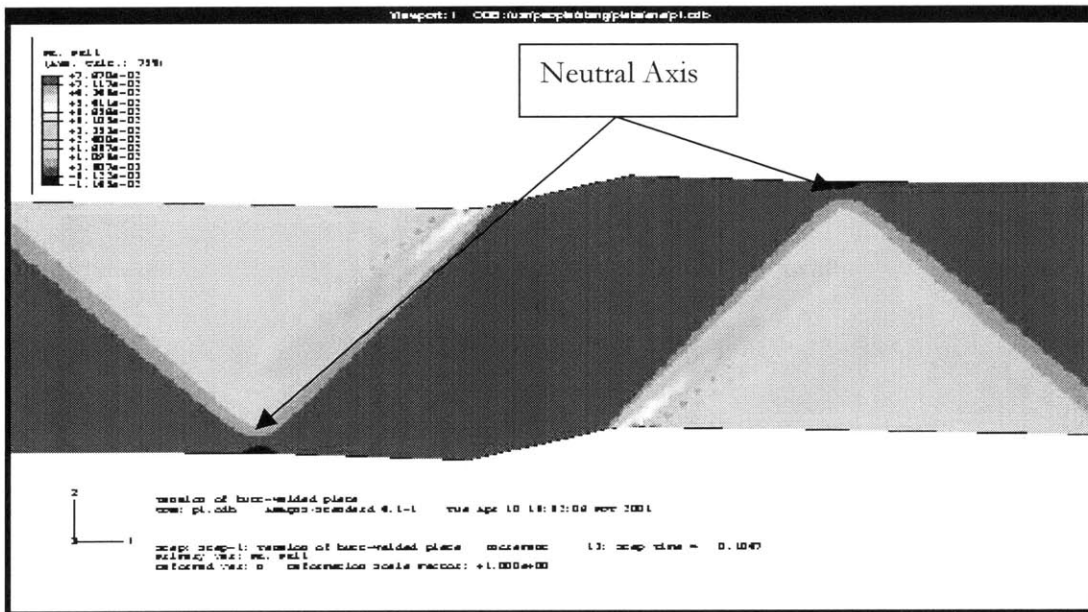


Figure 18. ABAQUS<sup>®</sup> displacement to onset of plasticity [13].  
 Edges of bands correspond to  $pe11 = \underline{-0.01}$  ( $0.007$ )  $\underline{+0.07}$

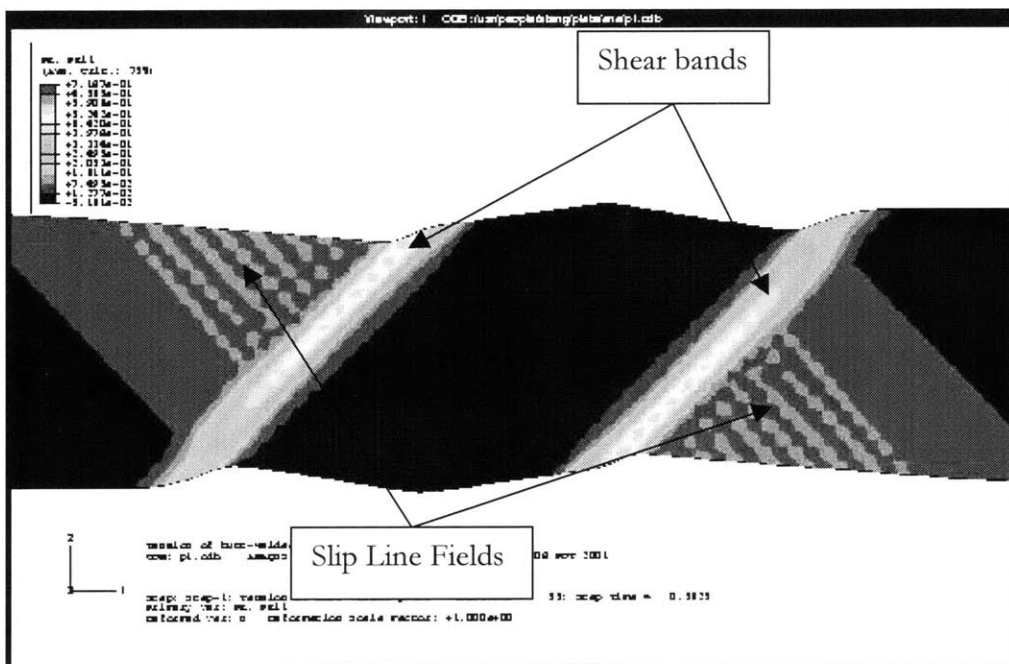


Figure 19. ABAQUS<sup>®</sup> showing slip line fields and shear bands [13].  
 Edges of bands correspond to  $p_{11} = \underline{-0.001}$  (0.05)  $\underline{+0.7}$ (Deformation exaggerated).

## Chapter 6 Experiments

### 6.1 Specimen design

In order to verify the results obtained from applying slip line field theory, it is necessary to design, build, and test specimens to observe the predicted phenomena. American Society of Test Mechanics, (ASTM), (2000) [14] does not specifically address how to design a test specimen for this particular application. Therefore, the flat tensile test specimen was used as guidance. It was necessary to determine the proper dimensions to ensure the testing machine was kept within its limitations. Appendix A shows the detailed calculations given the properties of EH-36 [9].

It was also necessary to carefully design the specimen utilizing existing test fixtures and jigs in order to mimic the effect of a far field tensile force being applied through the center of the weld for the duration of the test. Figure 20 shows the detailed geometry of the test specimen. It is believed the removed material (machined out region) on each side of the simulated weld keeps the tensile force, applied by the machine grips, acting through the center of the weld. Figure 21 shows a close-up view of the line of action of the applied force,  $P$ . A flush “dog-bone” test specimen, one with no offset, was used to verify the



material property data provided for EH-36 [9] and for subsequent input into ABACUS<sup>®</sup> for finite element analysis.

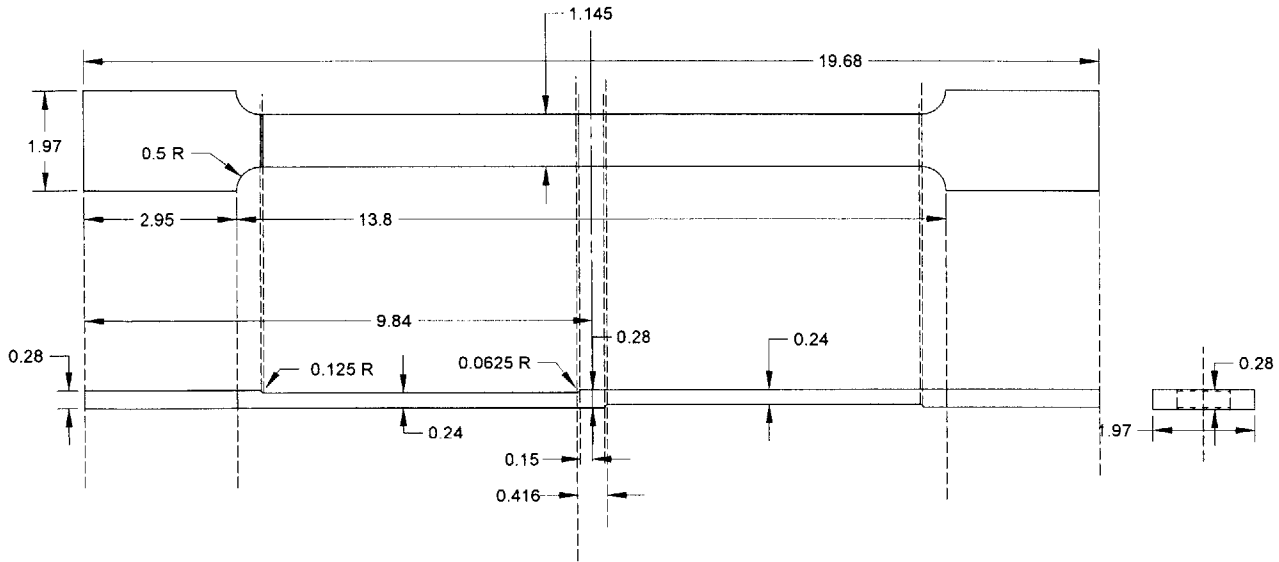


Figure 20. 16.7% offset test specimen drawing (dimensions in inches).

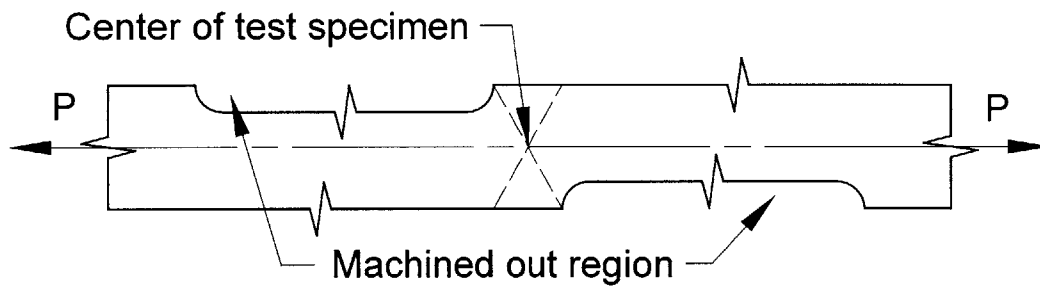


Figure 21. Cross-section of offset specimen showing the line of action.

(Not drawn to scale).

Actual welding of the test specimen was not performed because only the verification of slip line field theory was the phenomena that wanted to be studied at this point. It is

believed welding adds complexities and uncertainties unwanted at this phase of analysis. The predicted slip lines are still believed to be observable due to the fact the mid-section of the specimen is thicker and more massive than the adjacent machined out plates. Therefore, less stress and lower strains will be felt in the mid-section imitating a hard, rigid weld. Tests on welded plates with various degree of offset will be performed as a continuation of this research.

## 6.2 Testing procedure and apparatus

A MTS Model RF/200 floor standing testing machine was used to test the two specimens. First, the flat plate “dog-bone” specimen was placed vertically into the opposing grips. It was fitted with one extensometer near the midsection and the other extensometer on the same side in the top half of the specimen (see Figure 22). A steady displacement rate of 0.02 in/sec was applied to the top grip. The force on the load cell and the extensions were measured and recorded electronically. At maximum load, the extension was stopped and the upper extensometer was placed nearest the location of suspected failure to obtain a truer strain at failure. The extensometers were set-up to have a maximum extension of 0.2 inches or 50% strain.

The second test piece was machined as a “dog-bone” specimen with a 16.7% offset and the same thickness as the first specimen. Again, two extensometers were used (see Figure 23). One was placed next to the simulated weld on the tensile side on the upper half of the specimen within the expected active slip line field, while the other extensometer was placed on the same side approximately one-third of the way down from the top grip. To better view the results, the displacement rate applied to the top grip was slowed to

approximately 0.003 in/sec. Once necking was observed elsewhere the uni-axial stress was insufficient load to deform the specimen around the weld, the test was stopped.

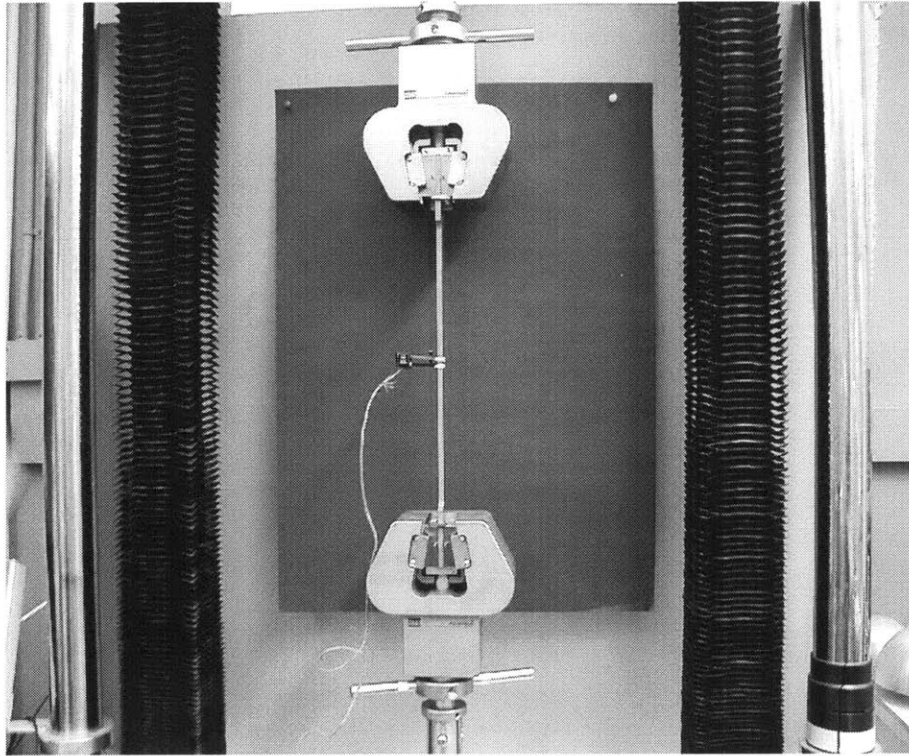


Figure 22. Test set-up of flat plate specimen. (Only one extensometer shown).

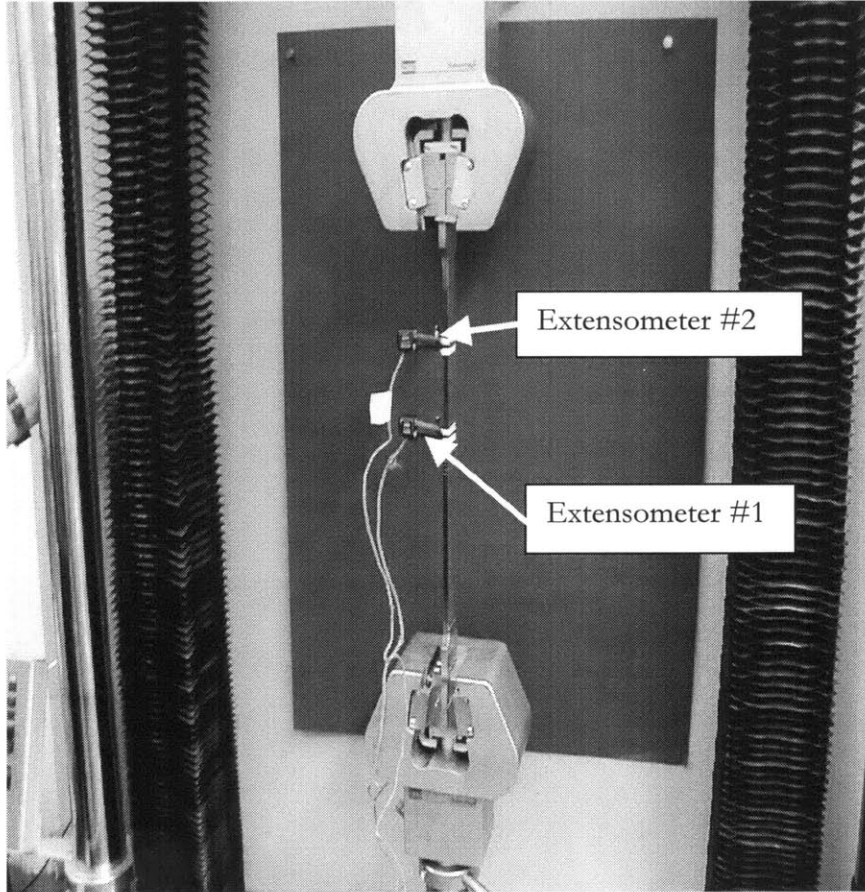


Figure 23. 16.7% offset test specimen set-up.

## Chapter 7 Analysis of test data

### 7.1 Results

The flat plate specimen exhibited typical mild steel properties. Figure 24 shows the stress-strain curve obtained for the tensile test. Appendix B contains the recorded data. Table 3 summarizes the material behavior of the flat plate tensile specimen pulled to failure. The discontinuity in the data is due to stopping the test and repositioning the second extensometer on the observed necking. At this point the first extensometer returns to its plastic strain value as its stress is unloaded.

Since the flat plate specimen failed at half the machine capacity, plane-strain conditions for the offset specimen would only require  $\frac{2}{\sqrt{3}}$ , or 15% greater load, well within the testing machine specifications.

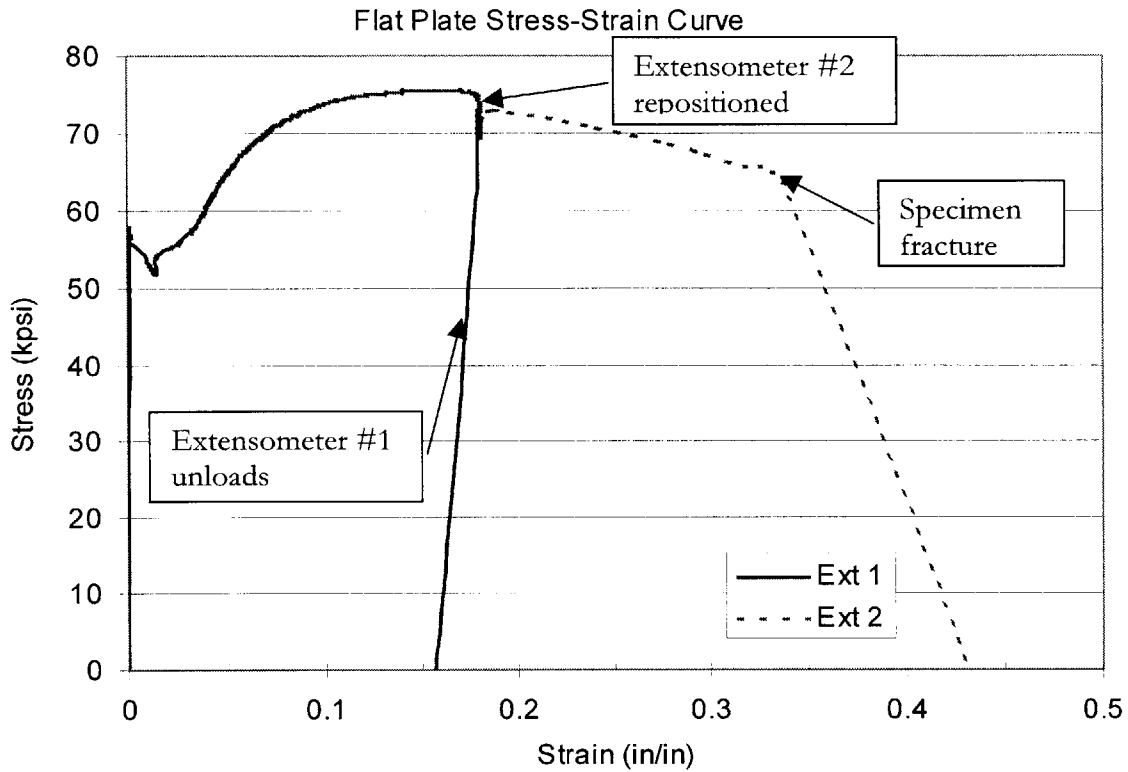


Figure 24. Stress-strain curve for the flat plate "dog-bone" specimen.

Table 3. Summary of observed properties of EH-36 specimens.

Property	Flat Plate Specimen	16.7% Offset Specimen
Upper Yield Point, UYP	56.6 kpsi	55.6 kpsi
Modulus of Elasticity, E	$34.5 \times 10^6$ psi	$49.1 \times 10^6$ psi
Tensile Strength, TS	75.5 kpsi	75.3 kpsi
Strain to Necking	0.157	0.155
Strain to Failure { $\ln (A_o/A)$ }	1.07	not observed

Table 3 also shows the material properties of the offset specimen compared to the initial flat plate specimen, while Figure 25 shows the stress-strain curve for the offset specimen. Appendix C contains the recorded data.

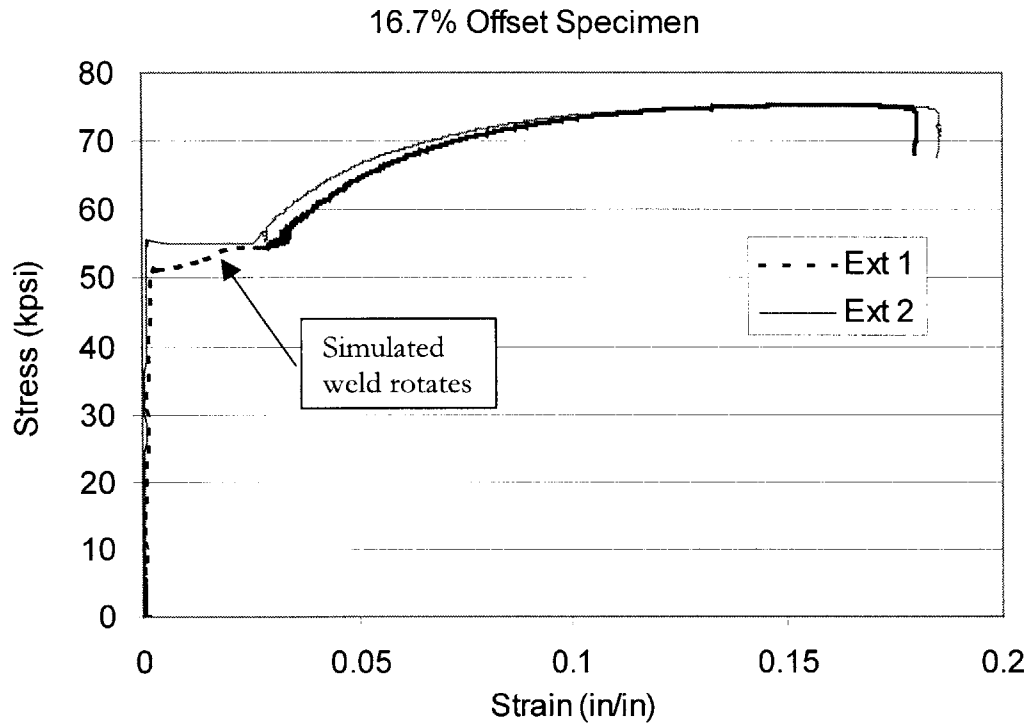


Figure 25. Stress-strain curve for specimen with 16.7% offset.

It was observed during testing of the offset specimen the simulated rigid weld region rotated as the material yielded (see Figure 26). The bend and thinning around the weld were insufficient to maintain plane-strain conditions. Post test measurements reveal the following comparisons summarized in Table 4. The simulated weld rotation, amount of strain, and the reduction in the plate thickness observed agrees with that predicted using slip line field theory.

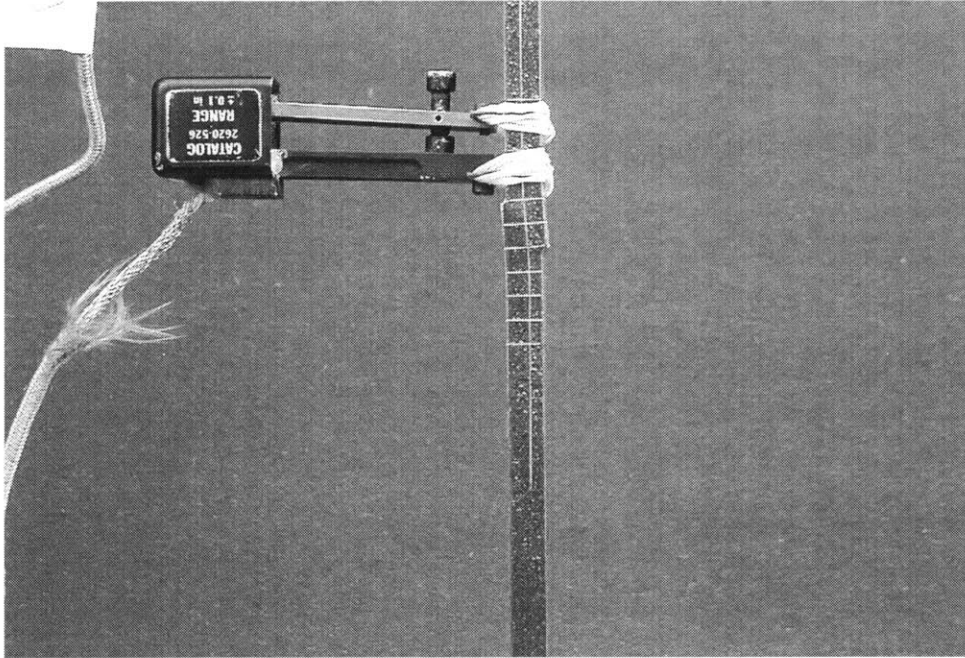


Figure 26. 16.7% offset specimen rotation.

Table 4. Comparison of test results to slip line field theory predictions.

Parameter	Slip Line Field Theory Prediction	Test Results
Simulated Weld region Rotation	4-6 degrees	4 degrees
Fraction of plate thickness reduction next to simulated weld region	0.046	0.07-0.104
Fractional strain on top surface next to simulated weld region	0.0303	0.03



## 7.2 Conclusions

Slip line field theory is a good tool to use in predicting the deformation and rigid body motions near an offset weld. Since the rotation of the simulated offset weld occurred in the lower yield region, it corresponded to slip line field theory. The assumption of plane-strain was not valid for the offset test specimen with a width-to-thickness ratio of 4. This led to the offset specimen necking away from the anticipated active slip field after rotation. Thus, the expected shearing fracture from the toe of the weld was not observed. One cannot ensure that for plane-strain service conditions the 16.7% offset would not diminish the strength. This conclusion should be revisited by testing additional specimens with shoulders to promote more nearly plane-strain and with much sharper transition regions (i.e. smaller fillet radii) to simulate the HAZ.

## 7.3 Recommendations for Further Study

This study should continue with actual welded specimens by a qualified shipyard with plain-strain and with the maximum offsets allowed by military standards [7]. Data recorded for the material behavior of EH-36 should be incorporated into ABAQUS<sup>®</sup> along with fracture criteria for more accurate finite element analysis. To facilitate the plane-strain condition assumed in slip line field theory, test specimens should have a width-to-thickness ratio of 10 in to the welded region while being wider elsewhere. Additionally, more detailed weldment hardness profiles should be conducted to capture the hardness gradient in the

HAZ. This may lead to a smaller fillet radius in the simulated weld to better model the hardness gradient.

Preliminary analysis for bending parallel to the weld shows no strain or stress enhancements and is believed to be of little consequence. However, bending along the length of the weld may introduce higher strains and should be explored.

Finally, a differential geometry solution should be sought that could be integrated for an approximate closed form solution.

## Bibliography

- [1] USS DONALD COOK (DDG-75) website, <http://www.spear.navy.mil/ships/ddg75>, Mar01.
- [2] Snelling, William A. (1946) "Direct Explosion Test for Welded Armor and Ship Plate: Prime and Welded Plate Tests", Ship Structure Committee Report 4.
- [3] Davis, Harmer E., G. E. Troxell, Earl R. Parker and A. Boodberg (1948) "Investigations of Brittle Cleavage Fracture of Welded Flat Plate by means of a Bend Test", Ship Structure Committee Report 6.
- [4] Dexter, R. J., E. B. Norris, W. R. Schick and P. D. Watson (1986) "Performance of Underwater Weldments", Ship Structure Committee Report 335.
- [5] Nguyen, T. Ninh, M. A. Wahab (1998) "The effect of weld geometry and residual stresses on the fatigue of welded joints under combined loading", Journal of Materials Processing Technology 77, pp. 201-208.
- [6] Cui, Weicheng, Zhengquan Wan and Alla E. Mansour (1999) "Steel concentration factor in plates with transverse butt-weld misalignment", Journal of Construction Steel Research 52, pp. 159-170.
- [7] MIL-STD-1689A(SH), Chapter 12, Table XIX.
- [8] Forrest, David (2001), personal correspondence, BIW.
- [9] Konkol, Paul J., Kenneth M. Sabo, Gerard P. Mercier, Keith R. Miller, Frederick D. Arnold (2000) "Evaluation of Forming, Flame Bending, and Welding of ABS Grade EH-36 Steel Plates", National Center for Excellence in Metalworking Technology, Limited distribution.
- [10] Shames, Irving H. (1989) "Introduction to Solid Mechanics", Prentice-Hall.
- [11] AVONDALE DRW No. C6-017 29-01-10 sheet 4 of 6.
- [12] Masubuchi, Koichi and R.G. Morris (2000) "A Welding Research and Engineering Festschrift", MIT Press.
- [13] Teng, Xiaoging (2001) "Numerical Simulation of Effects of Mismatch and Misfit on Response of Butt-welded Plates", MIT Impact and Crashworthiness Laboratory, Report #52.
- [14] ASTM (2000), Vol. 03.01, pp80.

## Appendix A Specimen calculations

Specimen dimension calculations for flat specimen:

Given:

Tensile Strength, TS of EH-36

$$TS = 78 \text{ kpsi}$$

MTS test machine rating of 200 kN (44961 lbs).

Design to use only one-half of MTS machine rating, F.

$$TS = \frac{P}{A}$$

$$A = wt$$

where A is the area, w is the specimen width, and t is the specimen thickness.

Solving for P,

$$P = A(TS) = (1.14 \text{ in})(0.24 \text{ in})(78000 \text{ lbs/in}^2)$$

$$P = 21340 \text{ lbs.}$$

$$\frac{P}{F} = \frac{21340 \text{ lbs}}{44961 \text{ lbs}} = 0.47$$

Thus the force, P, required to break the specimen is approximately one-half of the capability of the machine.

## Appendix B Flat plate specimen test data

Calibration Data:

Load channel (5000 lbs/volt)

Extensometer #1,  $f_c = 34.1192$  in/volt/volt

Extensometer #2,  $f_c = 32.0252$  in/volt/volt

Gage length = 0.4 in

Calculations:

$P = \text{Load}(5000 \text{ lbs/volt})$

$$\text{Extension (in)} = \frac{f_c}{\text{Input volts}} (\text{Ext 1 output volts})$$

$$\text{Strain} = \frac{\text{Extension}}{0.4}$$

Recorded Data

Time mark	Ext 1 (output volts)	Ext 2 (output volts)	Input volts	Load
1.21	0.012273	0.014064	3.99216	0.0329
2.96	0.012269	0.014069	3.99214	0.0329
122.42	0.013246	0.014035	4.00391	0.0377
124.17	0.013256	0.01403	4.00391	0.0377
125.89	0.01326	0.014019	4.00391	0.0377
127.64	0.013272	0.01403	4.0039	0.0377
129.34	0.013263	0.014028	4.0039	0.0377
131.09	0.01326	0.014028	4.0039	0.0377
132.8	0.013241	0.014019	4.00388	0.0377
162.25	0.013279	0.014045	4.00389	0.0377
164	0.013267	0.014045	4.00387	0.0377
165.75	0.013265	0.014047	4.00385	0.0377
167.46	0.013253	0.014052	4.00383	0.0279
169.21	0.013232	0.014042	4.00379	0.028
170.92	0.013232	0.014047	4.0037	0.2614
172.67	0.013217	0.014042	4.00349	0.6858
174.39	0.013232	0.014057	4.00316	1.1209
176.14	0.01322	0.014061	4.00267	1.6003
177.84	0.013172	0.014057	4.00211	2.074
179.59	0.013194	0.014057	4.00145	2.5722
181.3	0.013179	0.014069	4.00071	3.0241
183.05	0.013151	0.014047	3.99991	3.1109
184.76	0.013139	0.014035	3.99908	3.1049
186.51	0.013153	0.014052	3.99826	3.0992
188.23	0.013151	0.014052	3.99752	3.1465
189.98	0.013151	0.014057	3.99668	3.1137
191.68	0.013163	0.014047	3.99585	3.0829
193.44	0.013153	0.014057	3.99508	3.0685
195.19	0.013141	0.014052	3.99434	3.0952
196.91	0.013155	0.014057	3.99374	3.1041
198.66	0.013155	0.014057	3.99326	3.0969
200.37	0.013153	0.014047	3.99293	3.1644
202.12	0.013148	0.014069	3.99265	3.089
203.82	0.013141	0.014057	3.9925	3.1063
205.57	0.013158	0.01404	3.99226	3.0989
207.28	0.013155	0.014047	3.99213	3.0708
209.03	0.013165	0.014057	3.99212	3.0612
210.75	0.013175	0.014071	3.99215	3.0427
212.5	0.013158	0.014069	3.9922	3.0463

Time mark	Ext 1 (output volts)	Ext 2 (output volts)	Input volts	Load
214.21	0.01316	0.014061	3.99223	3.0539
215.96	0.013151	0.014061	3.99227	3.0513
219.41	0.012724	0.014057	3.99249	2.9197
221.12	0.012695	0.014061	3.99247	2.9083
222.89	0.012686	0.014061	3.99235	2.9003
224.64	0.012681	0.014066	3.99225	2.8953
226.34	0.012643	0.014066	3.99219	2.8904
228.09	0.01266	0.014071	3.99216	2.8855
229.8	0.012643	0.014057	3.9922	2.8807
231.55	0.012633	0.014045	3.99218	2.8772
233.26	0.012633	0.014061	3.99223	2.8758
235.01	0.012629	0.014061	3.99236	2.8727
236.73	0.012629	0.014057	3.9924	2.8709
238.48	0.012629	0.014057	3.99232	2.8709
240.18	0.012609	0.014061	3.99212	2.8661
241.93	0.012602	0.014057	3.99215	2.8661
243.64	0.0126	0.014052	3.99218	2.8661
245.39	0.0126	0.014052	3.99219	2.8612
247.1	0.012595	0.014057	3.99215	2.8612
248.87	0.012578	0.014064	3.99215	2.8612
250.62	0.012588	0.014057	3.99225	2.8612
252.32	0.012583	0.014061	3.99223	2.8574
254.07	0.012574	0.014076	3.99233	2.8563
255.78	0.012576	0.014057	3.99225	2.8563
257.53	0.012564	0.014052	3.99223	2.8563
259.25	0.012569	0.014057	3.99225	2.8563
261	0.012581	0.014061	3.99226	2.8563
262.71	0.012574	0.014061	3.99223	2.8514
319.32	0.012516	0.014052	3.99214	2.8368
321.03	0.012514	0.014057	3.99211	2.9619
322.78	0.012032	0.014042	3.9921	3.0479
324.5	0.01162	0.01404	3.9922	3.156
326.25	0.011506	0.014052	3.99223	3.2137
328	0.011439	0.014047	3.99224	3.2488
329.71	0.011365	0.014057	3.99227	3.2769
331.46	0.011336	0.014047	3.99223	3.3045
333.17	0.011301	0.014047	3.99218	3.3288
334.92	0.011246	0.014047	3.99217	3.3539
336.64	0.011198	0.014057	3.99217	3.3775
338.39	0.011165	0.014045	3.9921	3.4005
340.09	0.011112	0.014047	3.99213	3.4218
341.84	0.011067	0.014061	3.9921	3.4433
343.55	0.011026	0.014064	3.99211	3.4636
345.3	0.010986	0.014042	3.99211	3.4844
347.01	0.010943	0.014045	3.99215	3.5032
348.76	0.010893	0.014047	3.99215	3.5211
350.48	0.010867	0.014057	3.99218	3.5389
352.23	0.010812	0.014052	3.99219	3.5574
353.93	0.010781	0.014052	3.99214	3.5729
355.69	0.010728	0.014061	3.99206	3.5902
357.44	0.010688	0.014057	3.99205	3.6072
359.16	0.01064	0.014045	3.99215	3.6218
360.91	0.010588	0.014045	3.99219	3.6364
362.62	0.010561	0.014061	3.99216	3.651
364.37	0.010511	0.014052	3.99214	3.6656
366.07	0.010473	0.014052	3.99221	3.6786
367.82	0.010428	0.014047	3.99217	3.691
369.53	0.010397	0.014061	3.99221	3.7047
371.28	0.010349	0.014061	3.99231	3.7187
373	0.010299	0.014047	3.99238	3.7289
374.75	0.010247	0.014042	3.99232	3.7436
376.46	0.010218	0.014057	3.9923	3.7533
378.21	0.010175	0.014057	3.99233	3.7653
379.91	0.010111	0.014038	3.99233	3.7777
381.66	0.010087	0.014047	3.9923	3.7874
383.37	0.010046	0.014057	3.99227	3.7972
385.14	0.009999	0.014052	3.99216	3.8069
386.89	0.009946	0.014047	3.99217	3.8166
388.59	0.009913	0.014047	3.99216	3.8265

Time mark	Ext 1 (output volts)	Ext 2 (output volts)	Input volts	Load
390.34	0.009849	0.014047	3.99216	3.8362
392.05	0.009829	0.014052	3.99214	3.8459
395.51	0.009737	0.014052	3.99218	3.8654
397.26	0.009686	0.014045	3.99213	3.8726
398.98	0.009658	0.014047	3.99213	3.88
400.73	0.009624	0.014052	3.9921	3.8897
402.43	0.009558	0.014057	3.99206	3.896
404.18	0.009515	0.014061	3.99208	3.9044
405.89	0.009467	0.014052	3.99211	3.9127
407.64	0.009417	0.014061	3.99214	3.9191
409.35	0.009398	0.014064	3.99217	3.9261
411.1	0.009341	0.014061	3.9922	3.9337
412.82	0.009288	0.014057	3.99221	3.9386
414.57	0.009262	0.014057	3.99216	3.948
416.32	0.009207	0.014057	3.9922	3.9532
418.03	0.009155	0.014052	3.99222	3.9581
419.78	0.009105	0.014061	3.99225	3.9632
421.5	0.009064	0.014045	3.99229	3.9725
423.25	0.009009	0.014066	3.99225	3.9776
424.96	0.008978	0.014045	3.99227	3.9824
426.71	0.008921	0.01404	3.9923	3.9873
428.41	0.008885	0.014061	3.9923	3.9922
430.16	0.00884	0.014038	3.9923	3.9971
431.87	0.0088	0.014057	3.99221	4.0019
433.62	0.008745	0.01403	3.99214	4.0068
435.33	0.008711	0.01404	3.99215	4.0117
437.08	0.008664	0.014047	3.9922	4.0166
438.8	0.008623	0.01403	3.99218	4.0214
440.55	0.008583	0.014066	3.99222	4.0263
442.3	0.008525	0.014052	3.99222	4.0309
444.01	0.008504	0.014069	3.99221	4.0331
445.76	0.008449	0.014061	3.99218	4.0361
447.48	0.008406	0.014066	3.99215	4.0409
449.23	0.008358	0.014076	3.99223	4.0458
450.93	0.008316	0.014061	3.99225	4.0498
452.68	0.008261	0.014057	3.9922	4.0507
454.39	0.008208	0.014057	3.99221	4.0556
456.14	0.008177	0.014061	3.99223	4.0605
457.85	0.008127	0.014052	3.99221	4.0605
459.6	0.00807	0.014047	3.99223	4.0654
461.32	0.008034	0.014047	3.99219	4.0662
463.07	0.008006	0.014052	3.9922	4.0703
464.77	0.007946	0.014057	3.99219	4.0752
466.52	0.007905	0.014052	3.99223	4.0752
468.23	0.007853	0.014052	3.99223	4.08
470	0.007801	0.014052	3.99227	4.08
471.75	0.007755	0.014061	3.99218	4.0849
473.46	0.007708	0.014066	3.99221	4.0849
475.21	0.007677	0.014064	3.99217	4.0898
476.91	0.007617	0.014057	3.99214	4.0898
478.66	0.007579	0.014052	3.99217	4.0947
480.37	0.007526	0.014052	3.99217	4.0947
482.12	0.007472	0.014057	3.99215	4.0947
483.83	0.007431	0.014052	3.99212	4.0995
485.58	0.007383	0.014052	3.99215	4.0995
487.3	0.007336	0.014047	3.99221	4.1044
489.05	0.007286	0.01404	3.99221	4.1044
490.75	0.00724	0.014057	3.99224	4.1044
492.5	0.007205	0.014052	3.99221	4.1091
494.21	0.00715	0.014066	3.99219	4.1093
495.96	0.007107	0.014061	3.99225	4.1093
497.67	0.007052	0.014045	3.99226	4.1092
499.43	0.006999	0.014061	3.99225	4.1141
501.18	0.006949	0.014045	3.99229	4.1141
502.89	0.006904	0.014057	3.99224	4.1141
504.64	0.006861	0.014069	3.99218	4.1148
506.35	0.006823	0.014057	3.99217	4.1189
508.1	0.006752	0.014057	3.99217	4.1189
509.82	0.006723	0.014052	3.99215	4.1189

Time mark	Ext 1 (output volts)	Ext 2 (output volts)	Input volts	Load
511.57	0.006673	0.014047	3.99214	4.1189
513.27	0.006613	0.014057	3.99217	4.119
516.73	0.00652	0.014047	3.99209	4.1238
518.48	0.006461	0.014038	3.99212	4.1238
520.19	0.00642	0.014057	3.99213	4.1238
521.94	0.006384	0.014061	3.9921	4.1238
523.66	0.006339	0.014045	3.9921	4.1238
525.41	0.006287	0.014061	3.99208	4.1238
527.12	0.006237	0.014052	3.99209	4.1238
528.87	0.006186	0.014057	3.9921	4.1247
530.62	0.006129	0.014035	3.99207	4.1287
532.33	0.006086	0.014047	3.9921	4.1287
534.08	0.006036	0.014061	3.99215	4.1287
535.8	0.005986	0.014052	3.99215	4.1287
537.55	0.005931	0.014057	3.99211	4.1287
539.25	0.005881	0.014047	3.99212	4.1288
541	0.005819	0.014057	3.9921	4.1287
542.71	0.0058	0.014057	3.99218	4.1287
544.46	0.005736	0.014035	3.99215	4.1287
546.17	0.005691	0.014047	3.99214	4.1287
547.92	0.00564	0.014057	3.99208	4.1287
549.64	0.005605	0.014057	3.99212	4.1287
551.39	0.005555	0.014057	3.99211	4.1288
553.09	0.005514	0.014047	3.99209	4.1281
554.84	0.005457	0.014047	3.99213	4.1238
556.55	0.005419	0.014042	3.99208	4.1238
558.32	0.005388	0.014066	3.99201	4.1238
560.07	0.005335	0.014066	3.99203	4.1239
561.77	0.005295	0.014057	3.99204	4.1239
563.52	0.005249	0.014057	3.99207	4.1238
565.23	0.005209	0.014064	3.99209	4.1238
566.98	0.005156	0.014066	3.99213	4.119
568.69	0.00513	0.014052	3.99216	4.119
570.44	0.005078	0.014061	3.99213	4.119
572.16	0.00504	0.014069	3.99218	4.119
573.91	0.005018	0.014061	3.9922	4.1141
575.62	0.004978	0.014057	3.99216	4.1141
577.37	0.004925	0.014052	3.9922	4.1093
579.07	0.004906	0.014052	3.99217	4.1093
580.82	0.00487	0.014038	3.9921	4.1044
582.53	0.004842	0.014052	3.99218	4.1044
584.3	0.004825	0.014047	3.99222	4.0995
586.05	0.004808	0.01404	3.99229	4.0947
587.75	0.004785	0.014047	3.99233	4.0872
589.5	0.004751	0.014035	3.99231	4.08
591.21	0.004763	0.014045	3.99221	4.0703
592.96	0.004751	0.014035	3.99225	4.0572
594.67	0.004734	0.014033	3.99214	4.0426
596.42	0.004732	0.014028	3.99215	4.0246
598.14	0.00473	0.014028	3.99214	4.0029
599.89	0.00473	0.014026	3.99214	3.9781
601.59	0.004744	0.014047	3.99217	3.9498
603.34	0.004746	0.014026	3.99216	3.8539
605.05	0.004734	0.014042	3.99215	3.8289
606.8	0.004737	0.01403	3.99218	3.8166
608.51	0.004734	0.014035	3.99222	3.8117
610.26	0.004763	0.01404	3.9922	3.8069
830.19	0.004768	0.014004	3.99222	3.7923
831.94	0.00478	0.013999	3.99221	3.7923
833.66	0.004773	0.013999	3.9922	3.7923
835.41	0.004768	0.013988	3.99221	3.7923
837.12	0.004768	0.01399	3.99219	3.7923
838.87	0.004763	0.013995	3.99219	3.9027
840.57	0.004763	0.013628	3.99213	3.9905
842.33	0.004758	0.012755	3.99219	3.9565
844.08	0.004756	0.011858	3.99217	3.9144
845.8	0.004773	0.010995	3.99214	3.8669
847.55	0.004763	0.010046	3.99213	3.811
849.25	0.004763	0.009145	3.99216	3.7496



Time mark	Ext 1 (output volts)	Ext 2 (output volts)	Input volts	Load
851	0.004768	0.008175	3.9921	3.677
852.71	0.004773	0.007238	3.99217	3.5948
859.64	0.005877	0.000355	3.99215	-0.0364
861.39	0.006437	0.000355	3.99217	-0.0364
863.09	0.006437	0.00035	3.99218	-0.0364
864.84	0.006451	0.000369	3.99219	-0.0364
866.55	0.006437	0.000352	3.99218	-0.0364
868.3	0.006444	0.000369	3.99213	-0.0364
873.52	0.006432	0.000364	3.99217	-0.0364

## Appendix C Offset specimen test data

Calibration Data:

Load channel (5000 lbs/volt)

Extensometer #1,  $f_c = 34.1192$  in/volt/volt

Extensometer #2,  $f_c = 32.0252$  in/volt/volt

Gage length = 0.4 in

Calculations:

$P = \text{Load}(5000 \text{ lbs/volt})$

Extension (in) =  $\frac{f_c}{\text{Input volts}} (\text{Ext 1 output volts})$

Strain =  $\frac{\text{Extension}}{0.4}$

Recorded Data:

Time mark	Ext 1 (output volts)	Ext 2 (output volts)	Input volts	Load
1.2	0.013217	0.013761	4.003906	-0.00218
2.96	0.013222	0.013775	4.003922	-0.00219
226.18	0.013263	0.013861	4.003949	-0.00216
227.93	0.013241	0.013849	4.003937	-0.00217
229.64	0.013253	0.013854	4.003951	-0.00217
231.39	0.013263	0.013854	4.003958	-0.00217
233.1	0.013263	0.01384	4.003949	-0.00218
234.85	0.013263	0.013842	4.003934	-0.00216
236.57	0.013263	0.013854	4.003932	-0.00216
238.32	0.013265	0.013856	4.003906	-0.00217
240.02	0.013275	0.013856	4.003863	-0.00216
241.77	0.013253	0.013847	4.003829	0.017788
243.48	0.013251	0.013847	4.003734	0.082209
245.23	0.013241	0.013849	4.003524	0.11095
246.94	0.013248	0.013852	4.003279	0.130031
248.69	0.013241	0.013837	4.002842	0.161688
250.41	0.013256	0.013852	4.002342	0.209863
252.16	0.013256	0.013837	4.001762	0.277712
253.86	0.013251	0.013825	4.001162	0.356678
255.62	0.013217	0.013828	4.000504	0.454463
257.37	0.013222	0.013823	3.999857	0.565941
259.08	0.013227	0.013823	3.99913	0.681235
260.83	0.013227	0.013825	3.998472	0.811829
262.54	0.01321	0.013818	3.997759	0.94171
264.29	0.013203	0.013811	3.997085	1.079328
266	0.013196	0.013804	3.996434	1.216325
267.75	0.013191	0.013799	3.99579	1.358799
269.46	0.013172	0.013785	3.995234	1.499643
271.21	0.01317	0.013799	3.994739	1.646707
272.92	0.013191	0.013804	3.994297	1.78797
274.67	0.013186	0.013799	3.993856	1.927692
276.39	0.01317	0.013775	3.993513	2.08522
278.14	0.013165	0.013775	3.993132	2.23839
279.84	0.013158	0.013775	3.992855	2.387971
281.59	0.013158	0.013761	3.992731	2.54446
283.3	0.013139	0.013761	3.992681	2.687487
285.07	0.013098	0.013763	3.9926	2.794835
286.82	0.01286	0.013759	3.992576	2.836821

Time mark	Ext 1 (output volts)	Ext 2 (output volts)	Input volts	Load
288.52	0.012547	0.013763	3.992545	2.899522
290.27	0.012383	0.013763	3.992536	2.962398
291.98	0.012192	0.013775	3.992536	2.990188
293.73	0.012028	0.013773	3.992559	2.99777
295.44	0.011932	0.013773	3.992486	3.002622
297.19	0.011863	0.013754	3.992438	3.01505
298.91	0.011842	0.013754	3.992426	3.03668
300.66	0.011839	0.013773	3.992402	3.041512
302.36	0.011844	0.013775	3.992366	3.031799
304.11	0.01183	0.013775	3.992304	3.017225
305.82	0.011823	0.013759	3.992295	3.019695
307.57	0.011816	0.013761	3.992264	3.007431
309.28	0.011827	0.013756	3.992278	3.009023
311.03	0.011813	0.013763	3.9923	3.013629
312.75	0.011818	0.013763	3.992278	3.017241
314.5	0.011811	0.013766	3.992321	3.017232
316.25	0.011804	0.013768	3.992326	3.022086
317.96	0.011806	0.013763	3.99235	3.017225
319.71	0.011801	0.013761	3.992376	3.017227
321.42	0.011799	0.013761	3.992424	3.027865
323.17	0.011813	0.013773	3.992431	3.031783
324.89	0.011787	0.013761	3.992452	3.037171
326.64	0.011789	0.013756	3.992316	3.036189
328.34	0.011789	0.013761	3.992316	3.018887
330.09	0.011792	0.013768	3.99228	3.024859
331.8	0.011808	0.01378	3.992309	3.040792
333.55	0.011777	0.013759	3.992397	3.046436
335.26	0.01178	0.013763	3.992443	3.051328
337.01	0.011785	0.013761	3.992383	3.051335
338.73	0.011763	0.013775	3.992397	3.05624
340.48	0.011763	0.013771	3.992352	3.059685
342.23	0.011763	0.01378	3.992381	3.051345
343.94	0.011773	0.013751	3.992373	3.041524
345.69	0.011758	0.013768	3.99234	3.041517
347.41	0.011763	0.013775	3.992302	3.046441
349.16	0.011763	0.013766	3.992285	3.05135
350.86	0.011768	0.013768	3.992342	3.06113
352.61	0.011761	0.01378	3.992362	3.065981
354.32	0.011758	0.013763	3.992328	3.05135
356.07	0.011737	0.013761	3.992326	3.038148
357.78	0.011758	0.01378	3.992402	3.035509
359.53	0.011751	0.013759	3.992359	3.056247
361.25	0.011734	0.013525	3.99229	3.027851
363	0.011744	0.013017	3.992269	3.022177
364.7	0.011742	0.012717	3.992269	3.028681
366.45	0.011725	0.012547	3.992249	3.022136
368.16	0.011737	0.012502	3.99229	3.053753
369.92	0.011746	0.012481	3.992269	3.082778
371.67	0.011734	0.012462	3.992269	3.109724
373.39	0.011718	0.012428	3.992261	3.119456
375.14	0.011708	0.012435	3.992288	3.113193
376.84	0.011696	0.012414	3.992319	3.100025
378.59	0.011696	0.012388	3.992345	3.114602
380.3	0.011689	0.0124	3.992357	3.117346
382.05	0.011661	0.012388	3.992285	3.105435
383.76	0.011665	0.012383	3.992264	3.066165
385.51	0.011687	0.012385	3.992247	3.063442
387.23	0.01167	0.012397	3.992247	3.061125
388.98	0.011675	0.012404	3.992247	3.046138
390.68	0.011672	0.012395	3.992238	3.073656
392.43	0.011684	0.012376	3.992247	3.139832
394.14	0.011651	0.012376	3.992216	3.163416
395.89	0.011639	0.012362	3.992216	3.17811
397.6	0.011615	0.01234	3.992197	3.190329
399.36	0.011591	0.012321	3.992173	3.202443
401.11	0.011568	0.012316	3.992176	3.215327
402.82	0.011539	0.01229	3.992199	3.226866
404.57	0.011522	0.01228	3.992271	3.236629
406.28	0.011491	0.012249	3.992397	3.247778

Time mark	Ext 1 (output volts)	Ext 2 (output volts)	Input volts	Load
408.03	0.011465	0.012247	3.992304	3.256404
409.75	0.011446	0.012223	3.992362	3.265798
411.5	0.011446	0.012207	3.9924	3.275513
413.2	0.011425	0.012185	3.992319	3.283138
414.95	0.011401	0.012185	3.992273	3.290994
416.66	0.011398	0.01218	3.992304	3.301181
418.41	0.01137	0.012147	3.99228	3.313684
420.12	0.011367	0.012121	3.992285	3.324291
421.87	0.011365	0.012102	3.992311	3.334136
423.58	0.011329	0.012083	3.992264	3.343851
425.33	0.011327	0.01209	3.992278	3.353576
427.04	0.011303	0.012059	3.992271	3.363049
428.8	0.011281	0.01204	3.992261	3.373146
430.55	0.011258	0.012021	3.992321	3.381774
432.26	0.011239	0.011999	3.992311	3.389668
434.01	0.011212	0.011987	3.992333	3.398287
435.73	0.0112	0.011961	3.99228	3.407218
437.48	0.011179	0.011947	3.992264	3.416926
439.18	0.011184	0.011937	3.992333	3.42669
440.93	0.011155	0.011906	3.992311	3.43651
442.64	0.011146	0.011897	3.992328	3.441915
444.39	0.011117	0.01187	3.992321	3.451209
446.1	0.0111	0.011851	3.992302	3.460903
447.85	0.011072	0.011825	3.992309	3.469321
449.57	0.011062	0.011827	3.992352	3.475492
451.32	0.011053	0.011804	3.992342	3.485288
453.02	0.011022	0.011792	3.992471	3.492238
454.77	0.011014	0.011768	3.99244	3.499853
456.48	0.010986	0.011749	3.992443	3.509602
458.25	0.011	0.011732	3.992426	3.514511
460	0.010969	0.011718	3.992424	3.524324
461.7	0.010929	0.011699	3.9924	3.530366
463.45	0.010919	0.01167	3.992359	3.538899
465.16	0.010902	0.011656	3.992345	3.54428
466.91	0.01089	0.011634	3.992335	3.553459
468.62	0.010859	0.01162	3.992326	3.558685
470.37	0.01085	0.011591	3.992319	3.568131
472.08	0.01084	0.011577	3.992321	3.572945
473.83	0.010805	0.011563	3.992321	3.582644
475.54	0.01079	0.011541	3.992304	3.587591
477.29	0.010766	0.01151	3.992295	3.593239
479	0.010747	0.01151	3.992247	3.602352
480.75	0.010733	0.011496	3.992223	3.607208
482.46	0.010712	0.011477	3.992257	3.613412
484.23	0.010712	0.011451	3.992229	3.619229
485.98	0.010685	0.011439	3.992249	3.626701
487.68	0.010673	0.01142	3.992278	3.631503
489.43	0.010645	0.011394	3.992319	3.636386
491.14	0.010635	0.01137	3.992321	3.644356
492.89	0.010597	0.011346	3.992342	3.650979
494.6	0.010578	0.011329	3.99234	3.65585
496.35	0.010569	0.011327	3.992345	3.660757
498.07	0.010569	0.011308	3.99235	3.665692
499.82	0.010528	0.011281	3.992309	3.674721
501.52	0.010519	0.011277	3.992273	3.680329
503.27	0.010511	0.011243	3.992335	3.6852
504.98	0.010483	0.011231	3.992359	3.690016
506.73	0.010466	0.011196	3.992366	3.694899
508.44	0.010447	0.011184	3.992409	3.6998
510.19	0.010418	0.01116	3.992421	3.704695
511.91	0.010397	0.011141	3.992366	3.709998
513.66	0.010404	0.011136	3.992373	3.717706
515.41	0.010373	0.011105	3.99234	3.723318
517.12	0.010354	0.011096	3.992309	3.72895
518.87	0.010328	0.011055	3.992304	3.733854
520.58	0.010313	0.01105	3.992328	3.738741
522.33	0.010282	0.011019	3.992397	3.743605
524.04	0.010275	0.010993	3.992278	3.748159
525.79	0.010247	0.010964	3.992261	3.753108

Time mark	Ext 1 (output volts)	Ext 2 (output volts)	Input volts	Load
527.5	0.010232	0.010943	3.992245	3.758196
529.25	0.010197	0.010917	3.99219	3.762898
530.96	0.010194	0.010898	3.992197	3.76661
532.71	0.010178	0.010886	3.99218	3.769845
534.42	0.010161	0.010859	3.992271	3.773231
536.17	0.010132	0.01085	3.992304	3.777709
537.89	0.010123	0.010819	3.992295	3.782579
539.64	0.010101	0.010809	3.992285	3.787384
541.34	0.010077	0.010783	3.992319	3.792278
543.1	0.010063	0.010762	3.992311	3.797183
544.85	0.010032	0.010743	3.992321	3.802058
546.57	0.010027	0.010719	3.992362	3.806881
548.32	0.010001	0.0107	3.992376	3.808653
550.02	0.009992	0.010683	3.992311	3.811757
551.77	0.009961	0.01065	3.9923	3.816645
553.48	0.009942	0.010635	3.992321	3.821516
555.23	0.009927	0.010621	3.992383	3.826403
556.94	0.009908	0.010592	3.992319	3.831298
558.69	0.009903	0.01059	3.99228	3.833556
560.41	0.009875	0.010566	3.992311	3.836219
562.16	0.009858	0.01055	3.992352	3.841102
563.86	0.009856	0.010523	3.992326	3.845908
565.61	0.009818	0.010478	3.992328	3.849718
567.32	0.00981	0.010468	3.992381	3.850796
569.07	0.009779	0.010466	3.992397	3.855733
570.78	0.009772	0.010447	3.992359	3.86058
572.54	0.009756	0.010404	3.992316	3.864889
574.29	0.009713	0.010383	3.992288	3.86537
576	0.00972	0.010354	3.992264	3.870267
577.75	0.009694	0.01034	3.99223	3.875169
579.46	0.009667	0.010321	3.992183	3.875498
581.21	0.009658	0.010311	3.99229	3.880052
582.92	0.009636	0.010306	3.992271	3.884866
584.67	0.009608	0.010273	3.992288	3.887503
586.39	0.009601	0.010242	3.992481	3.889763
588.14	0.009586	0.010232	3.992502	3.894636
589.84	0.009551	0.010216	3.992426	3.895962
591.59	0.009534	0.010197	3.992452	3.899505
593.3	0.009524	0.010192	3.99244	3.904423
595.05	0.009498	0.010144	3.992426	3.904442
596.76	0.009467	0.010132	3.992393	3.909349
598.52	0.009465	0.010106	3.992614	3.914239
600.27	0.009438	0.010077	3.992536	3.914253
601.98	0.009419	0.010068	3.992433	3.919138
603.73	0.009405	0.010054	3.992359	3.921666
605.44	0.009386	0.010018	3.992397	3.923957
607.19	0.009357	0.009998	3.992328	3.928811
608.91	0.009341	0.009992	3.992342	3.928821
610.66	0.009319	0.009961	3.992223	3.93372
612.36	0.009307	0.009949	3.992223	3.933875
614.11	0.009288	0.009918	3.992166	3.938605
615.82	0.009269	0.009906	3.992187	3.941507
617.57	0.009238	0.00988	3.992168	3.943409
619.28	0.009222	0.009872	3.992192	3.94814
621.03	0.009212	0.009841	3.992173	3.948285
622.75	0.009193	0.00981	3.992173	3.953175
624.5	0.009181	0.009799	3.992023	3.953189
626.2	0.009148	0.00977	3.991951	3.958058
627.96	0.009138	0.009753	3.992078	3.958072
629.71	0.009109	0.009737	3.992137	3.962891
631.42	0.009105	0.00971	3.992149	3.9629
633.17	0.009078	0.009698	3.992156	3.967759
634.89	0.009059	0.009679	3.992142	3.96779
636.64	0.009031	0.009675	3.992168	3.972644
638.34	0.009026	0.009648	3.992214	3.972687
640.09	0.009016	0.009629	3.992209	3.977551
641.8	0.008997	0.009613	3.992209	3.97757
643.55	0.008974	0.009591	3.992137	3.982441
645.26	0.008947	0.00957	3.992149	3.982424

Time mark	Ext 1 (output volts)	Ext 2 (output volts)	Input volts	Load
647.01	0.008935	0.009543	3.99218	3.987178
648.73	0.008907	0.009531	3.992173	3.987343
650.48	0.008888	0.00951	3.992216	3.989598
652.18	0.008878	0.009477	3.992216	3.992221
653.93	0.008852	0.009458	3.992233	3.992223
655.64	0.008833	0.009438	3.992326	3.997123
657.41	0.008828	0.009436	3.992288	3.997128
659.16	0.008797	0.009403	3.992257	4.001908
660.86	0.00879	0.009369	3.992273	4.001932
662.61	0.008764	0.009377	3.992362	4.002571
664.32	0.00874	0.009357	3.992357	4.006817
666.07	0.008726	0.009326	3.99229	4.006843
667.78	0.008702	0.009295	3.99229	4.011721
669.53	0.008687	0.009293	3.992295	4.011752
671.25	0.008668	0.009269	3.99229	4.01369
673	0.008654	0.009255	3.992278	4.016599
674.7	0.008649	0.009238	3.992288	4.016609
676.45	0.008621	0.009205	3.99223	4.021399
678.16	0.008602	0.009181	3.992223	4.021382
679.91	0.00858	0.00916	3.992373	4.021399
681.62	0.008578	0.00915	3.992438	4.026279
683.37	0.008552	0.009136	3.992414	4.026315
685.08	0.008516	0.009105	3.992631	4.026873
686.84	0.008513	0.0091	3.992624	4.031176
688.59	0.008487	0.009071	3.992505	4.031178
690.3	0.008482	0.009045	3.992416	4.032154
692.05	0.008444	0.009024	3.992342	4.036066
693.76	0.008432	0.008997	3.992326	4.036056
695.51	0.008406	0.008974	3.992245	4.037592
697.23	0.008389	0.008957	3.992233	4.040887
698.98	0.008368	0.008935	3.992238	4.040884
700.68	0.008354	0.008909	3.992204	4.041371
702.43	0.008337	0.008885	3.992164	4.045767
704.14	0.008325	0.008883	3.992176	4.045767
705.89	0.008301	0.008873	3.992187	4.045774
707.6	0.008296	0.008838	3.992061	4.050676
709.35	0.008268	0.008838	3.992187	4.050676
711.07	0.008254	0.008809	3.992311	4.050679
712.82	0.008234	0.00878	3.992207	4.054746
714.52	0.008218	0.008759	3.992204	4.055552
716.28	0.008187	0.008733	3.992197	4.05555
718.03	0.008172	0.008716	3.992192	4.055719
719.75	0.008151	0.008692	3.992264	4.060506
721.5	0.008137	0.008678	3.992345	4.060506
723.2	0.008127	0.008654	3.992335	4.060504
724.95	0.008108	0.008645	3.992393	4.065005
726.66	0.008082	0.008628	3.992383	4.065406
728.41	0.008065	0.008599	3.99229	4.065403
730.12	0.008044	0.008575	3.992269	4.065401
731.87	0.008044	0.008549	3.992316	4.070303
733.58	0.008015	0.008552	3.992335	4.070303
735.33	0.007998	0.008509	3.992586	4.070293
737.04	0.007991	0.008499	3.99235	4.070334
738.79	0.007967	0.008471	3.992321	4.075174
740.5	0.007922	0.008454	3.992559	4.075183
742.26	0.007913	0.008413	3.992469	4.075186
744.01	0.007913	0.008423	3.992543	4.075183
745.73	0.007886	0.008394	3.992505	4.079856
747.48	0.007879	0.008375	3.992455	4.079995
749.18	0.007824	0.008351	3.99239	4.079999
750.93	0.007824	0.008342	3.992061	4.079999
752.64	0.007779	0.008301	3.992128	4.082145
754.39	0.007781	0.00828	3.99224	4.084887
756.1	0.00777	0.00827	3.992199	4.084894
757.85	0.00776	0.008246	3.992285	4.084904
759.57	0.007746	0.008227	3.99229	4.084908
761.32	0.007715	0.008208	3.992333	4.088308
763.02	0.0077	0.008177	3.992302	4.089784
764.77	0.007679	0.00817	3.992302	4.089813

Time mark	Ext 1 (output volts)	Ext 2 (output volts)	Input volts	Load
766.48	0.007665	0.008141	3.992321	4.089808
768.23	0.007655	0.008127	3.992333	4.089822
769.94	0.007615	0.008094	3.992357	4.092698
771.7	0.0076	0.008091	3.99239	4.09465
773.45	0.007598	0.008063	3.992357	4.094679
775.16	0.007567	0.008029	3.992381	4.094665
776.91	0.007545	0.00802	3.992373	4.094662
778.62	0.007529	0.007989	3.992421	4.094994
780.37	0.00751	0.007948	3.992321	4.099457
782.08	0.007488	0.007946	3.992328	4.099457
783.83	0.007469	0.007927	3.992424	4.09945
785.54	0.007445	0.007894	3.992519	4.099447
787.29	0.007433	0.007882	3.992502	4.09945
789	0.00741	0.00786	3.992605	4.101653
790.75	0.00741	0.007822	3.992536	4.10433
792.46	0.007379	0.007822	3.992512	4.104335
794.21	0.007355	0.007796	3.992443	4.104335
795.92	0.007345	0.00776	3.992383	4.104344
797.67	0.007326	0.007753	3.992352	4.104335
799.39	0.007302	0.007727	3.992381	4.104321
801.14	0.007286	0.007703	3.992362	4.107413
802.89	0.007269	0.007681	3.992316	4.109256
804.6	0.007252	0.007672	3.992333	4.109261
806.35	0.00724	0.00765	3.992302	4.109241
808.07	0.007209	0.007634	3.992269	4.109256
809.82	0.007195	0.007598	3.992245	4.109251
811.52	0.007178	0.007574	3.992304	4.109411
813.27	0.007164	0.007562	3.992311	4.113149
814.98	0.00715	0.007541	3.992261	4.114122
816.73	0.007114	0.007517	3.992319	4.114103
818.44	0.007107	0.007493	3.99224	4.114127
820.19	0.007083	0.007476	3.9923	4.114129
821.91	0.007061	0.007452	3.992316	4.114136
823.66	0.007042	0.007429	3.99235	4.114129
825.36	0.007033	0.007393	3.992397	4.114906
827.11	0.007014	0.007388	3.992362	4.118874
828.82	0.006995	0.007355	3.992321	4.118928
830.58	0.006985	0.007336	3.992209	4.118945
832.33	0.006966	0.007319	3.992199	4.118945
834.04	0.006959	0.007295	3.992273	4.118928
835.79	0.006926	0.007281	3.99234	4.118926
837.5	0.006899	0.007269	3.992328	4.118938
839.25	0.006887	0.007255	3.9923	4.118943
840.96	0.006861	0.007212	3.992285	4.118926
842.71	0.006849	0.007109	3.992257	4.123818
844.42	0.006814	0.007078	3.992285	4.12383
846.17	0.006809	0.007061	3.99229	4.123826
847.89	0.00678	0.007028	3.992273	4.123814
849.64	0.006775	0.007014	3.99228	4.123811
851.34	0.006756	0.006978	3.992288	4.123821
853.09	0.006742	0.006942	3.99228	4.123826
854.8	0.006721	0.006933	3.992304	4.12383
856.55	0.00669	0.00693	3.992309	4.123811
858.26	0.006673	0.006909	3.992295	4.123821
860.02	0.006663	0.006873	3.992359	4.124588
861.77	0.006659	0.006859	3.992342	4.127497
863.48	0.006647	0.006833	3.992319	4.128723
865.23	0.006611	0.006816	3.992288	4.128727
866.94	0.006594	0.00679	3.992254	4.12873
868.69	0.00658	0.006771	3.99224	4.12873
870.41	0.006568	0.006766	3.992309	4.128735
872.16	0.006568	0.006728	3.992288	4.12873
873.86	0.00653	0.006701	3.9923	4.128727
875.61	0.006504	0.006692	3.992328	4.12872
877.32	0.006499	0.006666	3.992328	4.128723
879.07	0.006482	0.006639	3.992319	4.12872
880.78	0.006458	0.00662	3.992311	4.12873
882.53	0.006442	0.006608	3.9923	4.12873
884.25	0.006437	0.00658	3.992273	4.128735

Time mark	Ext 1 (output volts)	Ext 2 (output volts)	Input volts	Load
886	0.006401	0.006554	3.992285	4.130837
887.75	0.006387	0.006515	3.992216	4.131724
889.46	0.00637	0.006499	3.992261	4.133617
891.21	0.006358	0.006496	3.992257	4.13361
892.92	0.006346	0.006468	3.992309	4.133605
894.67	0.006339	0.006446	3.992366	4.133613
896.39	0.006313	0.006418	3.992383	4.133613
898.14	0.006282	0.006399	3.992381	4.133601
899.84	0.006253	0.006384	3.992278	4.133617
901.59	0.006256	0.006356	3.992278	4.133603
903.3	0.006229	0.006334	3.9923	4.133601
905.05	0.006217	0.00631	3.992335	4.133589
906.76	0.006191	0.006289	3.992321	4.133603
908.51	0.006165	0.00626	3.992273	4.133613
910.23	0.006153	0.006241	3.992319	4.133591
911.98	0.006146	0.00621	3.992309	4.133601
913.68	0.006124	0.006203	3.992321	4.13361
915.44	0.006108	0.006177	3.992304	4.133586
917.19	0.006101	0.006153	3.992285	4.133603
918.91	0.00607	0.006124	3.992273	4.133596
920.66	0.006051	0.006115	3.992302	4.133596
922.36	0.006041	0.006105	3.992345	4.133586
924.11	0.006017	0.006067	3.992328	4.133601
925.82	0.006008	0.006058	3.992397	4.133601
927.57	0.006	0.006027	3.992433	4.133589
929.28	0.005981	0.005991	3.992414	4.133884
931.03	0.005979	0.005991	3.992385	4.135241
932.75	0.005941	0.005974	3.992407	4.134902
934.5	0.005939	0.005943	3.992383	4.135036
936.2	0.00591	0.005919	3.992319	4.135038
937.95	0.005898	0.0059	3.992335	4.135916
939.66	0.005865	0.005869	3.992309	4.136195
941.41	0.005853	0.005843	3.992233	4.137644
943.12	0.005826	0.005822	3.992245	4.136271
944.89	0.005817	0.005812	3.992321	4.13814
946.64	0.005815	0.005784	3.992359	4.137816
948.34	0.005791	0.005779	3.992352	4.137816
950.09	0.005767	0.00576	3.992383	4.137327
951.8	0.005748	0.005722	3.992295	4.137337
953.55	0.005724	0.0057	3.992278	4.13794
955.26	0.005736	0.005676	3.992224	4.137392
957.01	0.005693	0.005664	3.99229	4.13696
958.73	0.005667	0.005633	3.99228	4.137394
960.48	0.005664	0.005609	3.992381	4.137167
962.18	0.00564	0.005598	3.992288	4.137353
963.93	0.005629	0.005574	3.992247	4.135601
965.64	0.005629	0.00555	3.992326	4.135863
967.39	0.005595	0.005533	3.992543	4.133753
969.1	0.005581	0.005521	3.99265	4.133794
970.85	0.005564	0.005488	3.992552	4.133601
972.57	0.005559	0.005469	3.992402	4.133591
974.32	0.005521	0.005464	3.992366	4.133582
976.07	0.005526	0.005433	3.992309	4.133596
977.78	0.005502	0.005426	3.992309	4.133586
979.53	0.005481	0.005395	3.992257	4.133586
981.25	0.005452	0.005369	3.992288	4.133579
983	0.005431	0.005338	3.992264	4.133589
984.7	0.005426	0.005319	3.99228	4.133589
986.45	0.005421	0.005311	3.992247	4.133601
988.16	0.005414	0.005285	3.992335	4.133589
989.91	0.005388	0.005273	3.992373	4.133591
991.62	0.005369	0.005245	3.992278	4.133572
993.37	0.005345	0.005223	3.992233	4.133574
995.08	0.005345	0.005202	3.992125	4.133586
996.83	0.005323	0.005183	3.992209	4.133591
998.54	0.005319	0.005173	3.9923	4.133589
1000.29	0.00529	0.00514	3.992385	4.133582
1002	0.005266	0.005137	3.992285	4.133582
1003.76	0.005242	0.005099	3.992288	4.133572



Time mark	Ext 1 (output volts)	Ext 2 (output volts)	Input volts	Load
1005.51	0.005242	0.00508	3.992085	4.133586
1007.23	0.005214	0.005059	3.992209	4.133126
1008.98	0.005197	0.005044	3.9923	4.129796
1010.68	0.005187	0.005011	3.992385	4.128696
1012.43	0.00518	0.005006	3.992345	4.128696
1014.14	0.005173	0.004994	3.992335	4.128704
1015.89	0.005149	0.004961	3.992342	4.128723
1017.6	0.005145	0.004963	3.992311	4.128713
1019.35	0.005118	0.004916	3.992316	4.128713
1021.07	0.005106	0.004911	3.992488	4.128718
1022.82	0.005097	0.004904	3.992478	4.128723
1024.52	0.005078	0.004875	3.992352	4.12872
1026.27	0.005071	0.004866	3.992309	4.128077
1027.98	0.005047	0.004856	3.992328	4.123828
1029.75	0.005044	0.00483	3.99229	4.123828
1031.5	0.005028	0.004823	3.992316	4.123818
1033.2	0.005002	0.004801	3.992328	4.12383
1034.95	0.005002	0.004768	3.992309	4.123806
1036.66	0.004982	0.004754	3.992369	4.123818
1038.41	0.004982	0.004739	3.992362	4.123108
1040.12	0.004959	0.004732	3.992316	4.118921
1041.87	0.004959	0.004742	3.992383	4.118936
1043.58	0.004942	0.004715	3.992352	4.118936
1045.33	0.004925	0.004711	3.992335	4.118921
1047.04	0.004916	0.004682	3.992316	4.116573
1048.79	0.004894	0.004682	3.992311	4.114129
1050.5	0.004901	0.004668	3.992321	4.114108
1052.25	0.004882	0.004665	3.992326	4.113945
1053.96	0.004866	0.004651	3.992335	4.109239
1055.71	0.004875	0.004634	3.992342	4.109232
1057.42	0.004866	0.004639	3.99239	4.10434
1059.18	0.004849	0.004625	3.992393	4.104337
1060.93	0.004837	0.004613	3.992376	4.09944
1062.64	0.004842	0.004613	3.992373	4.09944
1064.39	0.004813	0.004599	3.992409	4.09466
1066.1	0.00482	0.004589	3.992373	4.090716
1067.85	0.004818	0.004599	3.992373	4.089765
1069.57	0.004813	0.004584	3.992424	4.08487
1071.32	0.004808	0.004575	3.992438	4.079983
1073.02	0.004808	0.004565	3.992376	4.075162
1074.77	0.004796	0.004575	3.99239	4.070267
1076.48	0.004799	0.004575	3.9924	4.061625
1078.23	0.004806	0.004572	3.992433	4.055557
1079.94	0.004792	0.004563	3.99244	4.049382
1081.69	0.004796	0.004568	3.992397	4.040884
1083.41	0.004801	0.004582	3.992385	4.031178
1085.16	0.004808	0.004582	3.992414	4.02373
1086.86	0.004796	0.004575	3.99239	4.01628
1088.62	0.004804	0.004582	3.992333	4.004576
1090.37	0.004799	0.004575	3.992316	3.99244
1092.08	0.004796	0.004553	3.992316	3.982417
1093.83	0.004799	0.004589	3.992261	3.972337
1095.54	0.004796	0.004584	3.992333	3.958072
1097.29	0.004808	0.004575	3.9923	3.946468
1099	0.004806	0.004558	3.99229	3.933722
1100.75	0.004794	0.004568	3.99223	3.919115
1102.46	0.004804	0.004553	3.992257	3.904428
1104.21	0.004808	0.004572	3.992321	3.888697
1105.92	0.004801	0.004568	3.992321	3.871698
1107.67	0.004806	0.004582	3.99239	3.855378
1109.39	0.00482	0.004575	3.992352	3.791966
1135.36	0.004823	0.004599	3.992328	3.724131